Quantitative Finance and Economics

https://www.aimspress.com/journal/QFE

QFE, 9(1): 202–241.
DOI: 10.3934/QFE.2025007
Received: 21 October 2024
Revised: 23 February 2025
Accepted: 13 March 2025
Published: 18 March 2025

Research article

Analysis of the trading interval duration for the Bitcoin market using high-frequency transaction data

Makoto Nakakita[1,*] **and Teruo Nakatsuma**[2]

[1] Center for Advanced Intelligence Project, RIKEN, Nihonbashi 1-Chome Mitsui Building, 15th Floor, 1-4-1 Nihonbashi, Chuo-ku, Tokyo, Japan

[2] Faculty of Economics, Keio University, 2-15-45 Mita, Minato-ku, Tokyo, Japan

* **Correspondence:** Email: nakakita.makoto@gmail.com, makoto.nakakita@riken.jp.

Abstract: Analyzing the trading interval durations of cryptocurrencies is important both academically and practically, but there has been no previous research using tick data. Therefore, we conducted a time series analysis on the duration of the trading interval between consecutive transactions in the Bitcoin market to identify similarities and differences with conventional financial assets such as stocks and commodities. We applied high-frequency transaction tick data from the Bitcoin market to a stochastic conditional duration (SCD) model and estimated the effects of trade price changes and volumes on the trading interval duration simultaneously with the intraday seasonality of the durations. As a result, we captured the effects of the direction of price movements and trading volume on trading interval durations. We also found that the trading interval duration is strongly persistent for Bitcoin similar to conventional financial assets. In contrast, we could not find any clear pattern of intraday seasonality for duration in the Bitcoin market.

Keywords: Bayesian methods; financial time series; high-frequency data; cryptocurrency; Markov chain Monte Carlo method; ancillary-sufficiency interweaving strategy; duration model

JEL Codes: C11, C15, C32, C41, G17

1. Introduction

Bitcoin is a digital currency first proposed by Nakamoto (2008) that is synonymous with cryptocurrencies, and it has by far the largest share of the market capitalization.[*] Bitcoin can be anonymously exchanged between users via peer-to-peer transactions, which are all recorded in a distributed digital ledger called a blockchain. As a result, Bitcoin is fully decentralized, and it is not

[*]Approximately 1.3 trillion US dollars at the time of writing.

controlled by any national governments, central banks, or other authorities. Since Bitcoin was released as open-source software and became operational in 2009, cryptocurrencies have drawn much attention for various reasons ranging from technological interest to financial speculation.

Bitcoin has been officially recognized as a currency in some regions. For example, Bitcoin was adopted as a fiat currency by the Republic of El Salvador in 2021 and the Central African Republic in 2022. Argentina designated Bitcoin as a currency that can be used for contractual agreements in 2023. In these cases, Bitcoin was adopted as a relatively safe currency by countries whose own fiat currency was hamstrung by hyperinflation, capital controls, or currency sanctions.

However, the anonymity and decentralized nature of Bitcoin has also led to it being used to purchase illegal drugs and for online gambling. For example, Christin (2013) estimated that Silk Road (i.e., a black-market site for illicit drug sales) once accounted for 4.5%–9% of Bitcoin circulation. It has also been pointed out that cryptocurrencies are at risk of being used for money laundering. To combat this problem, legitimate exchange services for trading cryptocurrencies and fiat currencies have enforced increasingly strict identity verification measures.

The increasing importance of cryptocurrencies has led to more research on them, among which price prediction has been one of the most active areas of research. Various methods have been employed for price prediction including machine learning (Chen, 2023; Derbentsev et al., 2020; Iqbal et al., 2021; McNallly et al., 2018; Ranjan et al., 2023), deep learning (Bouteska et al., 2024; Kim et al., 2022; Oyedele et al., 2023; Politis et al., 2021; Tanwar et al., 2021), statistical models (Georgoula et al., 2015; Maleki et al., 2023; Malladi and Dheeriya, 2021; Poongodi et al., 2020; Shah and Zhang, 2014), sentiment analysis using textual information from social networking sites, and index-based forecasting such as the Bitcoin Misery Index (Otabek and Choi, 2022; Hajek et al., 2023; Inuduka et al., 2024; Moustafa et al., 2022; Washington et al., 2023). In addition, systems for the automatic trading of cryptocurrencies based on predicted prices have been studied (Cohen, 2023; Jing and Kang, 2024; Khurana et al., 2023; Madan, 2014; Tran, 2023).

To the best of our knowledge, however, no studies have yet focused on the trading interval of cryptocurrencies. Although some studies have considered the volatility of cryptocurrencies, research on their trading intervals is still in its infancy compared to other financial assets. A negative relationship has been identified between the trading interval and return volatility in financial markets (Nakakita and Nakatsuma, 2021; Toyabe and Nakatsuma, 2022). Nakakita and Nakatsuma (2021) focused on the stock market and found that the intraday volatility of stock indices increased just after the market opened and just before it closed showing a U-shaped seasonality when plotted on a graph. In contrast, Toyabe and Nakatsuma (2022) analyzed the trading interval of individual Japanese stocks and found that the trading interval was shorter just after the market opened and just before it closed showing an inverse U-shaped seasonality.

These results indicate that previous studies on the volatility of cryptocurrencies may help with gaining insights into their trading interval. Chu et al. (2017) fitted various models to the daily price movements of cryptocurrencies and noted that they demonstrated very high volatility. Umar and Gubareva (2020) showed that COVID-19 had similar impacts on the market volatilities of cryptocurrencies and fiat currencies. Wang et al. (2023) used machine learning methods to predict the volatility of cryptocurrencies and showed that internal determinants (e.g., lagged volatility, previous trading information) were more important than external determinants (e.g., technology, financial, and policy uncertainty factors). These studies indicate that the volatility of cryptocurrencies has similar characteristics to that of financial instruments such as fiat currencies and equities, although there are some differences.

Research on the trading intervals of conventional financial instruments such as stocks and bonds has flourished since the late 1990s with the advent of the autoregressive conditional duration (ACD) model by Engle and Russell (1999). Prior to then, analyses of daily and monthly data were the mainstream, so the autoregressive conditional heteroskedasticity (ARCH) model (Engle, 1982) and generalized ARCH (GARCH) model (Bollerslev, 1986) assumed that trading intervals had a constant duration. However, as data storage technology advanced and data granularity reached timescales of minutes, seconds, and ticks, statistical models became necessary to overcome this traditional assumption. The ACD model was developed to handle data with nonuniform time intervals. Bauwens and Veredas (2004) proposed the stochastic conditional duration (SCD) model as an extension of the ACD model that can stochastically vary the duration and volatility. Strickland et al. (2006) further extended the SCD model to a Bayesian statistical framework to utilize the flexibility and estimation stability of Bayesian statistics, and this model has since been employed to analyze the durations of trading intervals in financial markets from both a frequentist and Bayesian perspective (Men et al., 2015; Thekke et al., 2016; Toyabe et al., 2024; Xu et al., 2010).

Based on the above literature, we analyzed the trading interval duration of the Bitcoin market. As there is no litereture on the trading interval duration of cryptocurrencies to the best of our knowledge, this research should be considered significant as it is pioneering in this area. Knowing the trading interval duration of financial instruments is helpful for understanding the number and attributes of market participants, which is useful not only for traders and other business practitioners but also for supervisory authorities to set up market regulations. For instance, understanding the patterns of trade interaval durations and the factors that influence them can help investors construct less risky portfolios and market managers operate their systems more robustly. We referred to previous studies (Nakakita and Nakatsuma, 2021; Toyabe et al., 2024) to develop a model that uses Bernstein polynomials to estimate intraday seasonality and control for trends that happen to occur on the day, which we hoped would accurately capture the relationship between each explanatory variable and the trading interval duration. This paper is expected to facilitate the expansion of research on trading interval durations to cryptocurrencies.

The rest of this paper is organized as follows. Section 2 describes the data used in this study. Section 3 presents the developed statistical model and the posterior distributions of the model parameters estimated by the Markov chain Monte Carlo (MCMC) method. Section 4 discusses the estimation results. Section 6 presents the conclusions.

2. Data

Tick data of spot trading between Bitcoin and US dollars were collected from the Binance website (Binance, 2024). At the time of writing, Binance is the world's largest Bitcoin exchange, and it has reported that the cumulative total of cryptocurrency trades reached 100 trillion dollars and the number of registered users reached 250 million (Binance, 2025). Here, spot trading was taken to refer to transactions in which financial instruments are exchanged at the current market rate. The data contained a history of all executed transactions, which could be used to examine the trading interval durations for Bitcoin. Transaction data for March and April 2024 were selected for this study because the data were the most recently available at the time of writing. By using data for two months, we aimed to ensure the robustness of our analysis. Data were only extracted each day for the 6.5-h period between 9:30 am and

4:00 pm. This is because March and April 2024 had more than 100,000,000 transactions in total, so the amount of data had to be limited to reduce computational costs. The 6.5-h period was selected to correspond with the trading hours of the US stock market. In addition, cryptocurrency exchanges are open 24 hours a day, 365 days a year, so traders can always trade on these markets. In contrast, stock markets are closed on weekends and over the New Year, etc. In this paper, we filtered the data according to trading hours, but we included weekends in the analysis. One of the aims of this paper is to examine whether there are differences between the market on weekdays and the market on weekends. As a result of data extraction, the number of executed trades used in the analysis came to 10,672,507 in March and 7,575,917 in April.

To facilitate analysis, the data were transformed by setting t as the time of day, where 9:30 corresponded to $t = 0$ and 16:00 corresponded to $t = 1$. Next, $\tau_{i,d}$ was taken as the i-th trading time of day d and $T_{i,d}$ was taken as the i-th trading interval duration of day d. Then, $T_{i,d}$ can be expressed as $T_{i,d} = \tau_{i+1,d} - \tau_{i,d}$, which obtained the explained variable $y_{i,d} = T_{i,d}/(24 \times 60 \times 60)$. Because the raw data were provided at a resolution of milliseconds, the trading interval duration could be analyzed with high accuracy. We created explanatory variables by processing information on the trade price, trade volume, and whether or not the maker is a buyer.† In the data, trade prices were available in cents, and trade volumes were available to the fifth decimal place. For this study, five explanatory variables were selected: the change in trade price, absolute value of the change in trade price, trade volume, change in trade price × trade volume, and absolute value of the change in trade price × trade volume.

Let $p_{i,d}$ and $v_{i,d}$ be the i-th trade price and trade volume, respectively, on day d. Then, the change in the i-th trade price can be expressed as $p_{i+1,d} - p_{i,d}$, and the i-th trade volume can be expressed as $v_{i+1,d}$. The descriptive statistics for the explained and explanatory variables are summarized in Tables 1 and 2. If the Bitcoin market is assumed to have the same characteristics as other financial markets in terms of changes in trade prices and volumes, then the regression coefficients for each explanatory variable can be expected as follows:

Log return: x_1

Financial markets are known to have a leverage effect, which can be defined as a negative relationship between the price change and volatility of financial instruments (Bollerslev et al., 2006; Omori et al., 2007; Nakakita and Nakatsuma, 2021). As we noted in Section 1, a negative relationship has also been observed between the volatility and trading interval duration. Therefore, the regression coefficient is expected to be positive.

Price increase dummy: x_2

There are three patterns for new transactions: price increase, no change, and price decrease. Since a price increase is thought to indicate that the market is fluctuating favorably, the regression coefficient will be negative.

Price decrease dummy: x_3

The price decrease may indicate that the market is fluctuating negatively. Although there are differences between strong and weak markets, both markets are active, so it can be hypothesized that the regression coefficient will be negative.

†Trading entities consist of makers and takers. Makers are entities that place orders at prices that are not on the order book and make up the liquidity of the order book. Takers place orders in response to orders on the order book and take liquidity from the order book because they are executed immediately.

Trade volume: x_4

The trade volume is considered to indicate the activity of a market. Because a large trade volume indicates an active market, it should correspond to a shorter trading interval duration, so the coefficient for this explanatory variable should be negative.

Price increase dummy × Trade volume: x_5

By multiplying the price increase dummy by the trade volume, we can see if the trading interval duration is affected not only by the direction of the price movement but also by its magnitude. We hypothesized that this explanatory variable has a positive coefficient due to the leverage effect.

Price increase dummy × Trade volume: x_6

While $x_{5,i}$ considers the effect when the price increases, this examines the effect of the trade volume when the price decreases. As with the previous variable, it is expected that the regression coefficient will be negative due to the leverage effect.

Absolute log return × Trade volume: x_7

This explanatory variable represents the monetary return of financial assets moved in a trade. Because the movement of large monetary value is considered indicative of the magnitude of movement in the market, the coefficient should be negative.

In addition to these five explanatory variables, we also added the term for intraday seasonality to control for trends that occurred during the day. A detailed description of intraday seasonality is given in Section 3.

Table 1. Descriptive statistics of explained and explanatory variables (March 2024).

Date	x_1				x_2				x_3				x_4			
	Mean	SD	Min	Max	Mean	SD	Min	Max	Mean	SD	Min	Max	Mean	SD	Min	Max
2024-03-01	-4.787×10^{-8}	1.365×10^{-5}	-7.314×10^{-4}	4.659×10^{-4}	0.193	0.395	0	1	0.196	0.397	0	1	2.444×10^{-3}	0.289	−22.45	22.81
2024-03-02	-4.347×10^{-9}	7.896×10^{-6}	-5.709×10^{-4}	3.684×10^{-4}	0.186	0.389	0	1	0.188	0.391	0	1	2.991×10^{-3}	0.123	−18.46	27.30
2024-03-03	2.248×10^{-8}	8.749×10^{-6}	-5.198×10^{-4}	2.441×10^{-4}	0.174	0.379	0	1	0.169	0.375	0	1	6.752×10^{-4}	0.278	−51.83	71.96
2024-03-04	4.232×10^{-8}	1.664×10^{-5}	-2.009×10^{-3}	1.164×10^{-3}	0.209	0.407	0	1	0.201	0.400	0	1	-3.669×10^{-3}	0.360	−59.66	42.11
2024-03-05	1.555×10^{-9}	5.445×10^{-5}	-7.831×10^{-3}	5.414×10^{-3}	0.215	0.411	0	1	0.212	0.409	0	1	3.792×10^{-4}	0.365	−61.16	56.73
2024-03-06	-1.527×10^{-8}	4.059×10^{-5}	-2.003×10^{-3}	2.003×10^{-3}	0.237	0.425	0	1	0.236	0.425	0	1	-5.667×10^{-4}	0.345	−57.92	74.75
2024-03-07	2.505×10^{-8}	2.062×10^{-5}	-9.290×10^{-4}	9.290×10^{-4}	0.209	0.407	0	1	0.204	0.403	0	1	-6.173×10^{-4}	0.381	−93.15	50.46
2024-03-08	1.274×10^{-8}	1.059×10^{-4}	-4.102×10^{-3}	3.513×10^{-3}	0.230	0.421	0	1	0.223	0.417	0	1	-5.941×10^{-3}	0.404	−96.70	35.52
2024-03-09	-4.765×10^{-9}	7.109×10^{-6}	-5.515×10^{-4}	3.735×10^{-4}	0.208	0.406	0	1	0.206	0.404	0	1	1.087×10^{-3}	0.150	−11.48	8.728
2024-03-10	-7.108×10^{-9}	1.406×10^{-5}	-1.820×10^{-3}	1.607×10^{-3}	0.200	0.400	0	1	0.196	0.397	0	1	1.374×10^{-3}	0.316	−43.25	72.11
2024-03-11	-1.051×10^{-9}	1.378×10^{-5}	-1.573×10^{-3}	9.193×10^{-4}	0.213	0.409	0	1	0.206	0.405	0	1	-1.932×10^{-3}	0.347	−98.25	53.50
2024-03-12	-9.308×10^{-9}	3.221×10^{-5}	-2.090×10^{-3}	2.058×10^{-3}	0.211	0.408	0	1	0.211	0.408	0	1	-1.108×10^{-2}	0.332	−51.22	44.35
2024-03-13	-2.857×10^{-8}	1.288×10^{-5}	-5.309×10^{-4}	5.440×10^{-4}	0.214	0.410	0	1	0.212	0.409	0	1	1.156×10^{-4}	0.305	−28.42	47.50
2024-03-14	-9.058×10^{-8}	1.790×10^{-5}	-1.700×10^{-3}	8.770×10^{-4}	0.227	0.419	0	1	0.238	0.426	0	1	1.220×10^{-3}	0.323	−39.07	45.98
2024-03-15	3.898×10^{-8}	3.047×10^{-5}	-1.886×10^{-3}	1.886×10^{-3}	0.244	0.430	0	1	0.245	0.430	0	1	6.534×10^{-4}	0.301	−42.50	31.33
2024-03-16	-3.036×10^{-8}	1.453×10^{-5}	-5.757×10^{-4}	6.139×10^{-4}	0.199	0.399	0	1	0.202	0.401	0	1	3.101×10^{-3}	0.242	−31.18	29.48
2024-03-17	67.54×10^{-8}	1.751×10^{-5}	-9.148×10^{-4}	1.162×10^{-3}	0.231	0.422	0	1	0.229	0.420	0	1	-1.626×10^{-3}	0.282	−58.17	26.90
2024-03-18	-3.214×10^{-8}	1.978×10^{-5}	-7.817×10^{-4}	5.119×10^{-4}	0.238	0.426	0	1	0.236	0.425	0	1	3.773×10^{-4}	0.266	−30.26	25.04
2024-03-19	1.426×10^{-8}	2.414×10^{-5}	-1.142×10^{-3}	8.843×10^{-4}	0.226	0.418	0	1	0.235	0.424	0	1	-2.659×10^{-3}	0.369	−72.27	40.93
2024-03-20	-1.794×10^{-8}	2.016×10^{-5}	-9.485×10^{-4}	8.837×10^{-4}	0.252	0.434	0	1	0.240	0.427	0	1	3.612×10^{-3}	0.298	−29.96	31.24
2024-03-21	-3.505×10^{-8}	2.552×10^{-5}	-4.749×10^{-4}	2.861×10^{-3}	0.258	0.437	0	1	0.263	0.440	0	1	-4.597×10^{-3}	0.381	−11.89	29.09
2024-03-22	-8.428×10^{-8}	2.429×10^{-5}	-8.485×10^{-4}	6.691×10^{-4}	0.248	0.432	0	1	0.259	0.438	0	1	3.038×10^{-4}	0.360	−96.85	28.09
2024-03-23	5.609×10^{-8}	1.777×10^{-5}	-6.773×10^{-4}	5.907×10^{-4}	0.234	0.423	0	1	0.230	0.421	0	1	1.015×10^{-3}	0.275	−39.83	25.42
2024-03-24	6.520×10^{-8}	1.444×10^{-5}	-8.422×10^{-4}	5.293×10^{-4}	0.227	0.419	0	1	0.216	0.411	0	1	1.138×10^{-3}	0.327	−41.33	34.97
2024-03-25	1.214×10^{-7}	2.187×10^{-5}	-1.939×10^{-3}	1.407×10^{-3}	0.243	0.429	0	1	0.232	0.422	0	1	-4.442×10^{-3}	0.409	−50.00	49.85
2024-03-26	-3.406×10^{-8}	1.686×10^{-5}	-7.505×10^{-4}	1.054×10^{-3}	0.239	0.427	0	1	0.247	0.431	0	1	-1.918×10^{-3}	0.302	−45.29	28.07
2024-03-27	-3.220×10^{-8}	3.468×10^{-5}	-3.232×10^{-3}	2.552×10^{-3}	0.215	0.411	0	1	0.221	0.415	0	1	-1.931×10^{-3}	0.418	−51.37	66.60
2024-03-28	-2.997×10^{-8}	1.434×10^{-5}	-5.533×10^{-4}	5.501×10^{-4}	0.232	0.422	0	1	0.216	0.412	0	1	-3.393×10^{-3}	0.357	−79.64	37.96
2024-03-29	-4.561×10^{-8}	1.474×10^{-5}	-1.358×10^{-3}	7.661×10^{-4}	0.230	0.421	0	1	0.227	0.419	0	1	9.357×10^{-4}	0.370	−65.71	42.90
2024-03-30	-7.659×10^{-9}	5.668×10^{-6}	-6.274×10^{-4}	2.285×10^{-4}	0.199	0.399	0	1	0.199	0.399	0	1	-6.580×10^{-4}	0.216	−26.95	10.00
2024-03-31	8.790×10^{-9}	6.917×10^{-6}	-4.909×10^{-4}	5.474×10^{-4}	0.199	0.399	0	1	0.190	0.392	0	1	2.555×10^{-3}	0.268	−31.42	40.23

Presented values for the trading interval duration are after data transformation.

Table 1. Descriptive statistics of explained and explanatory variables (March 2024) (continued).

Date	x_5 Mean	x_5 SD	x_5 Min	x_5 Max	x_6 Mean	x_6 SD	x_6 Min	x_6 Max	x_7 Mean	x_7 SD	x_7 Min	x_7 Max
2024-03-01	-1.057×10^{-2}	0.176	−13.46	22.81	1.125×10^{-2}	0.189	−22.45	19.34	1.373×10^{-6}	5.239×10^{-5}	0	1.642×10^{-2}
2024-03-02	-6.431×10^{-3}	0.113	−18.46	27.30	6.244×10^{-3}	0.158	−44.18	17.84	6.326×10^{-7}	-6.127×10^{-5}	0	2.299×10^{-2}
2024-03-03	-6.366×10^{-2}	0.212	−51.83	71.96	6.342×10^{-3}	0.154	−27.68	20.27	6.724×10^{-7}	-3.306×10^{-5}	0	1.112×10^{-2}
2024-03-04	-9.207×10^{-3}	0.219	−42.00	42.11	8.534×10^{-3}	0.241	−59.66	29.66	2.138×10^{-6}	1.872×10^{-4}	0	1.012×10^{-1}
2024-03-05	-8.977×10^{-3}	0.264	−61.16	56.73	9.891×10^{-3}	0.215	−44.70	39.46	4.270×10^{-6}	-6.460×10^{-4}	0	3.373×10^{-1}
2024-03-06	-1.157×10^{-2}	0.231	−37.02	74.75	1.177×10^{-2}	0.230	−57.92	30.53	2.961×10^{-6}	1.563×10^{-4}	0	7.031×10^{-2}
2024-03-07	-1.136×10^{-2}	0.287	−93.15	50.46	1.118×10^{-2}	0.211	−36.75	19.94	2.071×10^{-6}	1.106×10^{-4}	0	3.999×10^{-2}
2024-03-08	-1.213×10^{-2}	0.210	−46.52	23.56	1.061×10^{-2}	0.256	−51.87	43.52	4.290×10^{-6}	3.559×10^{-4}	0	1.858×10^{-1}
2024-03-09	-5.670×10^{-3}	0.084	−7.895	8.695	6.766×10^{-3}	0.093	−11.48	8.728	3.432×10^{-7}	1.113×10^{-5}	0	2.491×10^{-3}
2024-03-10	-7.706×10^{-3}	0.216	−20.65	72.11	8.790×10^{-3}	0.196	−43.25	30.49	1.492×10^{-6}	1.532×10^{-4}	0	6.052×10^{-2}
2024-03-11	-1.050×10^{-2}	0.179	−29.06	53.50	9.998×10^{-3}	0.218	−50.09	49.46	1.711×10^{-6}	-1.775×10^{-4}	0	7.814×10^{-2}
2024-03-12	-1.108×10^{-2}	0.199	−30.20	44.35	1.051×10^{-2}	0.227	−51.22	26.68	2.768×10^{-6}	-2.886×10^{-4}	0	1.024×10^{-1}
2024-03-13	-9.775×10^{-3}	0.182	−28.15	47.50	1.060×10^{-2}	0.198	−28.42	28.47	1.323×10^{-6}	-6.741×10^{-5}	0	2.254×10^{-2}
2024-03-14	-1.280×10^{-2}	0.181	−21.99	45.98	1.362×10^{-2}	0.232	−39.07	45.44	1.925×10^{-6}	-1.486×10^{-4}	0	7.723×10^{-2}
2024-03-15	-1.273×10^{-2}	0.203	−42.50	24.81	1.368×10^{-2}	0.185	−39.94	31.33	1.952×10^{-6}	8.719×10^{-5}	0	4.670×10^{-2}
2024-03-16	-8.278×10^{-2}	0.143	−12.65	29.33	1.038×10^{-2}	0.168	−31.18	29.48	9.970×10^{-7}	-4.395×10^{-5}	0	1.386×10^{-2}
2024-03-17	-1.031×10^{-2}	0.203	−58.17	26.90	9.989×10^{-3}	0.165	−51.48	14.12	1.808×10^{-6}	-1.595×10^{-4}	0	6.757×10^{-2}
2024-03-18	-1.216×10^{-2}	0.168	−16.21	25.04	1.244×10^{-2}	0.178	−30.26	20.88	1.569×10^{-6}	4.570×10^{-5}	0	1.556×10^{-2}
2024-03-19	-1.453×10^{-2}	0.235	−72.27	40.93	1.355×10^{-2}	0.235	−46.64	34.99	2.734×10^{-6}	1.204×10^{-4}	0	4.438×10^{-2}
2024-03-20	-9.922×10^{-3}	0.188	−27.56	31.24	1.115×10^{-2}	0.202	−29.96	30.02	1.930×10^{-6}	6.173×10^{-5}	0	1.400×10^{-2}
2024-03-21	-1.262×10^{-2}	0.181	−29.74	29.09	1.103×10^{-2}	0.319	−11.89	23.69	4.496×10^{-6}	-8.966×10^{-4}	0	3.252×10^{-1}
2024-03-22	-1.295×10^{-2}	0.197	−20.28	28.09	1.260×10^{-2}	0.275	−96.85	20.16	3.049×10^{-6}	1.572×10^{-4}	0	7.678×10^{-2}
2024-03-23	-8.189×10^{-3}	0.185	−24.67	24.62	8.078×10^{-3}	0.182	−39.83	25.42	1.720×10^{-6}	8.183×10^{-5}	0	2.042×10^{-2}
2024-03-24	-7.660×10^{-3}	0.248	−41.33	34.97	8.058×10^{-3}	0.170	−37.57	19.99	1.631×10^{-6}	-8.974×10^{-5}	0	3.165×10^{-2}
2024-03-25	-1.338×10^{-2}	0.261	−31.27	38.73	1.227×10^{-2}	0.281	−50.00	49.85	3.490×10^{-6}	2.558×10^{-5}	0	9.663×10^{-2}
2024-03-26	-9.812×10^{-3}	0.208	−45.19	28.07	9.544×10^{-3}	0.188	−31.90	20.53	1.872×10^{-6}	8.166×10^{-5}	0	2.508×10^{-2}
2024-03-27	-1.084×10^{-2}	0.285	−51.37	66.60	9.726×10^{-3}	0.277	−47.76	28.70	4.344×10^{-6}	-3.190×10^{-4}	0	1.176×10^{-1}
2024-03-28	-1.037×10^{-2}	0.266	−79.64	37.96	8.949×10^{-3}	0.200	−43.34	22.21	1.533×10^{-6}	6.503×10^{-5}	0	2.398×10^{-2}
2024-03-29	-9.391×10^{-3}	0.146	−17.36	22.04	9.445×10^{-3}	0.319	−65.71	42.90	2.643×10^{-6}	2.719×10^{-4}	0	8.925×10^{-2}
2024-03-30	-4.942×10^{-3}	0.104	−19.89	8.089	3.470×10^{-3}	0.176	−26.95	10.00	6.797×10^{-7}	6.583×10^{-5}	0	1.691×10^{-2}
2024-03-31	-5.424×10^{-3}	0.195	−31.42	40.23	7.089×10^{-3}	0.148	−19.89	14.96	7.470×10^{-7}	4.131×10^{-5}	0	8.040×10^{-3}

Presented values for the trading interval duration are after data transformation.

Table 2. Descriptive statistics of explained and explanatory variables (April 2024).

	x_1				x_2				x_3				x_4			
Date	Mean	SD	Min	Max	Mean	SD	Min	Max	Mean	SD	Min	Max	Mean	SD	Min	Max
2024-04-01	-7.577×10^{-8}	1.562×10^{-5}	-5.678×10^{-4}	5.280×10^{-4}	0.223	0.416	0	1	0.227	0.419	0	1	-1.554×10^{-3}	0.318	−29.42	25.06
2024-04-02	-4.242×10^{-8}	2.184×10^{-5}	-1.339×10^{-3}	1.122×10^{-3}	0.240	0.427	0	1	0.246	0.431	0	1	-2.921×10^{-3}	0.550	−99.95	71.16
2024-04-03	-3.646×10^{-8}	1.718×10^{-5}	-8.815×10^{-4}	6.612×10^{-4}	0.242	0.428	0	1	0.243	0.429	0	1	-1.727×10^{-3}	0.343	−57.85	39.03
2024-04-04	-8.054×10^{-8}	1.361×10^{-5}	-6.815×10^{-4}	8.326×10^{-4}	0.223	0.417	0	1	0.205	0.404	0	1	-7.078×10^{-3}	0.431	−36.46	82.59
2024-04-05	-7.987×10^{-8}	2.000×10^{-5}	-1.639×10^{-3}	1.090×10^{-3}	0.237	0.425	0	1	0.230	0.421	0	1	-5.637×10^{-3}	0.394	−76.71	62.69
2024-04-06	-1.260×10^{-8}	1.115×10^{-5}	-1.726×10^{-3}	9.378×10^{-4}	0.184	0.387	0	1	0.183	0.386	0	1	1.733×10^{-3}	0.421	−95.74	42.01
2024-04-07	1.749×10^{-8}	1.016×10^{-5}	-5.723×10^{-4}	5.591×10^{-4}	0.221	0.415	0	1	0.223	0.416	0	1	-2.313×10^{-3}	0.221	−25.91	27.15
2024-04-08	-1.996×10^{-8}	1.279×10^{-5}	-1.521×10^{-3}	5.780×10^{-4}	0.203	0.402	0	1	0.200	0.400	0	1	-8.428×10^{-3}	0.290	−70.40	24.85
2024-04-09	-6.736×10^{-8}	1.988×10^{-5}	-1.991×10^{-3}	8.247×10^{-4}	0.225	0.417	0	1	0.226	0.418	0	1	-2.748×10^{-3}	0.483	−85.34	39.17
2024-04-10	-2.240×10^{-8}	2.519×10^{-5}	-2.615×10^{-3}	2.474×10^{-3}	0.226	0.418	0	1	0.230	0.420	0	1	-3.167×10^{-3}	0.419	−59.49	48.11
2024-04-11	-4.053×10^{-8}	1.546×10^{-5}	-5.523×10^{-4}	6.597×10^{-4}	0.221	0.415	0	1	0.222	0.416	0	1	-1.886×10^{-3}	0.363	−36.15	64.65
2024-04-12	-6.546×10^{-8}	1.216×10^{-5}	-5.269×10^{-4}	9.101×10^{-4}	0.179	0.383	0	1	0.180	0.384	0	1	8.208×10^{-3}	0.363	−27.01	51.03
2024-04-13	-3.693×10^{-8}	1.148×10^{-5}	-4.418×10^{-4}	4.418×10^{-4}	0.230	0.421	0	1	0.220	0.414	0	1	3.234×10^{-3}	0.230	−37.25	47.33
2024-04-14	-9.220×10^{-9}	2.187×10^{-5}	-2.358×10^{-3}	1.966×10^{-3}	0.243	0.429	0	1	0.241	0.428	0	1	-4.104×10^{-3}	0.499	−102.4	49.87
2024-04-15	-1.064×10^{-7}	1.964×10^{-5}	-2.034×10^{-3}	1.483×10^{-3}	0.243	0.429	0	1	0.241	0.428	0	1	-3.107×10^{-3}	0.380	−76.17	35.10
2024-04-16	-6.716×10^{-8}	1.997×10^{-5}	-7.066×10^{-4}	6.082×10^{-4}	0.235	0.424	0	1	0.234	0.423	0	1	1.662×10^{-3}	0.259	−35.18	33.94
2024-04-17	-1.298×10^{-7}	2.549×10^{-5}	-1.635×10^{-3}	1.335×10^{-3}	0.236	0.424	0	1	0.251	0.433	0	1	2.231×10^{-3}	0.395	−56.61	49.99
2024-04-18	9.425×10^{-8}	2.219×10^{-5}	-9.366×10^{-4}	1.705×10^{-3}	0.236	0.425	0	1	0.225	0.417	0	1	2.880×10^{-3}	0.492	−84.05	72.83
2024-04-19	-9.239×10^{-9}	2.481×10^{-5}	-2.365×10^{-3}	1.614×10^{-3}	0.245	0.430	0	1	0.241	0.428	0	1	-2.962×10^{-3}	0.404	−62.42	51.17
2024-04-20	1.250×10^{-7}	1.475×10^{-5}	-1.270×10^{-3}	5.125×10^{-4}	0.239	0.427	0	1	0.235	0.424	0	1	-1.462×10^{-3}	0.337	−85.58	33.10
2024-04-21	1.279×10^{-8}	9.776×10^{-6}	-3.170×10^{-4}	3.208×10^{-4}	0.220	0.414	0	1	0.227	0.419	0	1	-1.218×10^{-3}	0.183	−15.78	14.14
2024-04-22	2.794×10^{-9}	1.117×10^{-5}	-4.003×10^{-4}	4.226×10^{-4}	0.242	0.428	0	1	0.234	0.424	0	1	1.801×10^{-3}	0.263	−45.61	30.86
2024-04-23	-1.469×10^{-8}	1.220×10^{-5}	-6.024×10^{-4}	6.024×10^{-4}	0.214	0.410	0	1	0.210	0.408	0	1	8.734×10^{-4}	0.332	−44.71	30.43
2024-04-24	-1.029×10^{-7}	1.915×10^{-5}	-9.469×10^{-4}	1.296×10^{-3}	0.228	0.420	0	1	0.235	0.414	0	1	-9.536×10^{-4}	0.376	−51.99	71.01
2024-04-25	7.622×10^{-9}	1.718×10^{-5}	-6.729×10^{-4}	6.630×10^{-4}	0.250	0.433	0	1	0.250	0.433	0	1	5.818×10^{-4}	0.352	−38.40	50.54
2024-04-26	-8.295×10^{-8}	1.807×10^{-5}	-2.605×10^{-3}	1.973×10^{-3}	0.260	0.438	0	1	0.262	0.440	0	1	-3.605×10^{-3}	0.626	−110.7	76.61
2024-04-27	-1.738×10^{-9}	1.176×10^{-5}	-4.060×10^{-4}	1.175×10^{-3}	0.228	0.420	0	1	0.226	0.418	0	1	-6.078×10^{-3}	0.397	−15.84	86.09
2024-04-28	-4.037×10^{-8}	1.179×10^{-5}	-8.909×10^{-4}	8.453×10^{-4}	0.239	0.426	0	1	0.242	0.429	0	1	2.262×10^{-3}	0.273	−17.62	24.67
2024-04-29	7.031×10^{-8}	1.402×10^{-5}	-4.949×10^{-4}	9.569×10^{-4}	0.252	0.434	0	1	0.257	0.427	0	1	-3.968×10^{-4}	0.397	−35.24	46.41
2024-04-30	-6.283×10^{-8}	2.435×10^{-5}	-2.125×10^{-3}	1.290×10^{-3}	0.221	0.415	0	1	0.231	0.421	0	1	-7.645×10^{-3}	0.482	−97.02	32.89

Presented values for the trading interval duration are after the data transformation.

Table 2. Descriptive statistics of explained and explanatory variables (April 2024) (continued).

Date	x_5 Mean	x_5 SD	x_5 Min	x_5 Max	x_6 Mean	x_6 SD	x_6 Min	x_6 Max	x_7 Mean	x_7 SD	x_7 Min	x_7 Max
2024-04-01	-1.173×10^{-2}	0.156	−12.88	12.43	1.101×10^{-2}	0.234	−29.42	25.06	1.621×10^{-6}	4.564×10^{-5}	0	6.854×10^{-3}
2024-04-02	-1.243×10^{-2}	0.359	−99.95	52.20	1.218×10^{-2}	0.360	−67.65	71.16	4.448×10^{-6}	2.659×10^{-4}	0	9.055×10^{-2}
2024-04-03	-9.308×10^{-3}	0.239	−57.85	38.97	9.324×10^{-3}	0.222	−39.35	39.03	1.929×10^{-6}	1.166×10^{-4}	0	3.468×10^{-2}
2024-04-04	-6.300×10^{-3}	0.332	−21.07	82.59	8.657×10^{-3}	0.237	−36.46	46.19	2.476×10^{-6}	1.864×10^{-4}	0	4.232×10^{-2}
2024-04-05	-1.109×10^{-2}	0.280	−76.71	62.69	8.018×10^{-3}	0.254	−45.85	57.37	3.043×10^{-6}	2.679×10^{-4}	0	9.400×10^{-2}
2024-04-06	-3.324×10^{-3}	0.253	−25.29	42.01	3.434×10^{-3}	0.312	−95.74	13.78	2.780×10^{-6}	4.345×10^{-4}	0	1.653×10^{-1}
2024-04-07	-7.799×10^{-3}	0.140	−25.91	13.71	6.551×10^{-3}	0.141	−19.56	27.15	7.994×10^{-7}	4.322×10^{-5}	0	1.037×10^{-2}
2024-04-08	-1.098×10^{-2}	0.200	−70.40	24.85	7.943×10^{-3}	0.183	−55.03	23.35	1.429×10^{-6}	1.426×10^{-4}	0	8.370×10^{-2}
2024-04-09	-1.091×10^{-2}	0.241	−49.58	39.17	8.351×10^{-3}	0.391	−85.34	26.68	3.862×10^{-6}	4.204×10^{-4}	0	1.699×10^{-1}
2024-04-10	-9.745×10^{-3}	0.251	−22.43	46.26	1.098×10^{-2}	0.294	−59.49	48.11	3.518×10^{-6}	2.368×10^{-4}	0	7.020×10^{-2}
2024-04-11	-8.585×10^{-3}	0.272	−29.97	64.65	9.342×10^{-3}	0.208	−36.15	25.39	2.194×10^{-6}	1.252×10^{-4}	0	3.749×10^{-2}
2024-04-12	-5.622×10^{-3}	0.266	−8.961	51.03	9.328×10^{-3}	0.195	−27.01	31.87	2.219×10^{-6}	-1.759×10^{-4}	0	3.677×10^{-2}
2024-04-13	-6.402×10^{-3}	0.155	−37.25	31.57	7.422×10^{-3}	0.154	−56.45	47.33	6.912×10^{-7}	3.325×10^{-5}	0	9.371×10^{-3}
2024-04-14	-1.203×10^{-2}	0.209	−41.33	49.87	1.065×10^{-2}	0.427	−102.4	42.59	5.327×10^{-6}	6.307×10^{-4}	0	2.415×10^{-1}
2024-04-15	-1.071×10^{-2}	0.157	−32.13	15.12	9.082×10^{-3}	0.319	−76.17	35.10	3.057×10^{-6}	3.243×10^{-4}	0	1.550×10^{-1}
2024-04-16	-9.316×10^{-3}	0.150	−19.83	33.94	1.039×10^{-2}	0.180	−35.18	18.57	1.695×10^{-6}	6.392×10^{-5}	0	2.268×10^{-2}
2024-04-17	-1.026×10^{-2}	0.230	−14.76	49.99	1.133×10^{-2}	0.291	−56.61	41.24	3.274×10^{-6}	2.002×10^{-4}	0	9.257×10^{-2}
2024-04-18	-9.264×10^{-3}	0.387	−84.05	72.83	1.033×10^{-2}	0.266	−53.81	44.56	4.266×10^{-6}	3.112×10^{-4}	0	8.085×10^{-2}
2024-04-19	-1.213×10^{-2}	0.265	−39.84	51.17	1.112×10^{-2}	0.271	−62.42	29.34	4.004×10^{-6}	3.458×10^{-4}	0	1.196×10^{-1}
2024-04-20	-9.271×10^{-3}	0.187	−22.88	33.10	7.512×10^{-3}	0.264	−85.58	21.23	1.940×10^{-6}	2.835×10^{-4}	0	1.087×10^{-1}
2024-04-21	-7.887×10^{-3}	0.123	−15.78	14.14	6.867×10^{-3}	0.097	−10.31	10.45	6.323×10^{-7}	1.686×10^{-5}	0	2.833×10^{-3}
2024-04-22	-9.426×10^{-3}	0.180	−45.61	20.32	1.038×10^{-2}	0.161	−25.49	30.86	9.718×10^{-7}	3.666×10^{-5}	0	7.925×10^{-3}
2024-04-23	-9.897×10^{-3}	0.239	−44.71	30.43	1.012×10^{-2}	0.187	−30.30	24.47	1.588×10^{-6}	7.818×10^{-5}	0	1.563×10^{-2}
2024-04-24	-1.139×10^{-2}	0.273	−48.20	71.01	1.088×10^{-2}	0.226	−51.99	34.77	2.614×10^{-6}	2.552×10^{-4}	0	8.441×10^{-2}
2024-04-25	-1.403×10^{-2}	0.194	−25.86	20.06	1.429×10^{-2}	0.259	−38.40	50.54	1.950×10^{-6}	6.768×10^{-5}	0	1.625×10^{-2}
2024-04-26	-1.305×10^{-2}	0.315	−30.41	76.61	1.067×10^{-2}	0.518	−110.7	51.30	6.439×10^{-6}	8.295×10^{-4}	0	2.807×10^{-1}
2024-04-27	-5.971×10^{-3}	0.331	−15.84	86.09	9.714×10^{-3}	0.186	−15.00	15.08	2.778×10^{-6}	3.316×10^{-4}	0	1.012×10^{-1}
2024-04-28	-1.008×10^{-2}	0.174	−17.62	9.977	1.047×10^{-2}	0.182	−10.69	24.67	1.346×10^{-6}	6.360×10^{-5}	0	1.255×10^{-2}
2024-04-29	-1.327×10^{-2}	0.291	−35.24	46.41	1.477×10^{-2}	0.232	−20.53	35.75	2.470×10^{-6}	1.428×10^{-4}	0	4.441×10^{-2}
2024-04-30	-1.244×10^{-2}	0.209	−23.93	32.89	8.479×10^{-3}	0.398	−97.02	26.41	5.795×10^{-6}	4.540×10^{-4}	0	9.519×10^{-2}

Presented values for the trading interval duration are after the data transformation.

3. Model

3.1. Proposed model

In this section, we describe our proposed model for trading interval durations in the Bitcoin market and derive the posterior distributions of the model parameters for estimation by the MCMC method. Our proposed model is based on the SCD model:

$$y_i = \exp(x_i'\beta + \alpha_i)\,\varepsilon_i, \quad \varepsilon_i > 0, \quad i \in \{1, \ldots, N\}, \tag{1}$$

$$\begin{aligned} \alpha_i &= \phi\alpha_{i-1} + \eta_i, \quad \eta_i \sim \text{Normal}(0, \sigma^2), \quad i \in \{2, \ldots, N\}, \\ \alpha_1 &\sim \text{Normal}(0, \sigma^2/(1-\phi^2)), \quad |\phi| < 1, \end{aligned} \tag{2}$$

where both ε_i and η_i are mutually and serially independent. The SCD model is a nonlinear non-Gaussian state-space model where Equation (1) is the observation equation and Equation (2) is the state equation. Note that all parameters should have the subscript d for the date, but they are omitted here for the sake of readability. x_i is a vector of the explanatory variables, and β is a vector of the corresponding regression coefficients. For x_i, in addition to the five variables described in Section 2, a term for the intraday seasonality is included in the form of a Bernstein polynomial to control for trends that occurred during the day. The n-th-order Bernstein basis function is expressed as

$$b_{v,n}(x) = \binom{n}{v} x^v (1-x)^{n-v}, \quad v = 0, \ldots, n. \tag{3}$$

Linear combination of these basis functions results in the Bernstein polynomial:

$$x_i^{IS\prime}\beta^{IS} = \sum_{v=0}^{n} \beta_v^{IS} x_{v,i} = \sum_{v=0}^{n} \beta_l^{IS} b_{v,n}(t_i). \tag{4}$$

The Bernstein polynomial has been proven to approximate any continuous function as n is increased to infinity (Bernstein, 1912). Summing up for $\boldsymbol{x_i}$ obtains $\boldsymbol{x_i} = [b_{i1}\ b_{i2}\ b_{i3}\ b_{i4}\ b_{i5}\ b_{i6}\ b_{i7}\ x_i^{IS\prime}]'$. Then, we can estimate the regression coefficients of the explanatory variables, intraday seasonality, and other parameters simultaneously.

We performed the estimation separately for each day from April 1 to April 30, 2024, to test whether the Bitcoin market differed in characteristics depending on the day. We used the deviance information criterion (DIC) proposed by Spiegelhalter et al. (2002) to select the appropriate order of the Bernstein polynomial for each day.

For ε_i in Equation (1), we set the Weibull distribution expressed by the probability density function (PDF) as follows:

$$p(\varepsilon_i|\gamma) = \gamma\varepsilon_i^{\gamma-1}\exp(-\varepsilon_i^{\gamma}). \tag{5}$$

The PDF of y_i is given by

$$p(y_i|\alpha_i, \beta, \gamma, \boldsymbol{x}_i) = \gamma y_i^{\gamma-1}\exp\left(-\gamma(x_i'\beta + \alpha_i) - y_i^{\gamma}\exp(-\gamma(x_i'\beta + \alpha_i))\right). \tag{6}$$

Because Equation (2) is a stationary first-order autoregressive model (AR(1) model), the joint probability distribution of $\boldsymbol{\alpha} = [\alpha_1 \dots \alpha_n]'$ is given by

$$\boldsymbol{\alpha} = \text{Normal}(\mathbf{0}, \sigma^2 V^{-1}), \tag{7}$$

$$V = \begin{bmatrix} 1 & -\phi & & & & & \\ -\phi & 1+\phi^2 & -\phi & & & & \\ & -\phi & 1+\phi^2 & -\phi & & & \\ & & \ddots & \ddots & \ddots & & \\ & & & -\phi & 1+\phi^2 & -\phi & \\ & & & & -\phi & 1+\phi^2 & -\phi \\ & & & & & -\phi & 1 \end{bmatrix}. \tag{8}$$

V is a tridiagonal matrix, and it is positive definite so long as $|\phi| < 1$ holds. Given the above settings, the prior distributions of the parameters $(\boldsymbol{\beta}, \gamma, \phi, \sigma^2)$ are given by

$$\begin{aligned} &\boldsymbol{\beta} \sim \text{Normal}(\boldsymbol{\mu}_\beta, \Sigma_\beta^{-1}), \quad \gamma \sim \text{Gamma}(a_\gamma, b_\gamma), \\ &\frac{\phi+1}{2} \sim \text{Beta}(a_\phi, b_\phi), \quad \sigma^2 \sim \text{Inv. Gamma}(a_\sigma, b_\sigma), \end{aligned} \tag{9}$$

where $\text{Gamma}(a_\gamma, b_\gamma)$ denotes a gamma distribution with the shape parameter a_γ and rate parameter b_γ, $\text{Beta}(a_\phi, b_\phi)$ denotes a beta distribution with the shape parameters a_ϕ and b_ϕ, and $\text{Inv. Gamma}(a_\sigma, b_\sigma)$ denotes an inverse gamma distribution with the shape parameter a_σ and scale parameter b_σ.

Then, the joint posterior distribution of $(\alpha, \beta, \gamma, \phi, \sigma^2)$ for Equations (1) and (2) is given by

$$p(\alpha, \beta, \gamma, \phi, \sigma^2 | \boldsymbol{y}, X) \propto \prod_{i=1}^{n} p(y_i | \alpha_i, \beta, \gamma, \boldsymbol{x}_i) p(\alpha | \phi, \sigma^2) p(\beta) p(\gamma) p(\phi) p(\sigma^2), \tag{10}$$

$$\boldsymbol{y} = [y_1 \ \dots \ y_n]', \quad X = [\boldsymbol{x}_1 \ \dots \ \boldsymbol{x}_n]', \tag{11}$$

where $p(y_i|\alpha_i, \beta, \gamma)$ is the PDF of the Weibull distribution in Equation (5). Because the joint posterior distribution in Equation (10) cannot be estimated analytically, we employed the MCMC method to estimate the distribution numerically.

For simplicity of notation, let $\theta = (\boldsymbol{\beta}, \gamma, \phi, \sigma^2)$. Then, we need to derive the conditional posterior distributions of the parameters in order to perform the MCMC method. The derivation of the conditional posterior distributions is complex and requires various mathematical techniques. Hence, the details are described in the appendix.

4. Empirical analysis and results

We conducted an empirical analysis where we established four candidates for the dimensional order of the Bernstein polynomial representing the intraday seasonality: 3, 7, 11, and 15. The prior distribution was set as follows:

$$\boldsymbol{\beta} \sim \text{Normal}(\mathbf{0}, I), \quad \gamma \sim \text{Gamma}(3, 10),$$
$$\frac{\phi + 1}{2} \sim \text{Beta}(20, 1), \quad \sigma^2 \sim \text{Inv. Gamma}(3, 10),$$

where I is the identity matrix.

The number of iterations for MCMC sampling was set to 1000 for the sampling period and 100 for the burn-in period. We utilized Geweke's convergence diagnostic to confirm convergence of the samples, and we extended the burn-in period if Geweke's convergence diagnostic did not pass at the 1% level for all parameters. For example, if the number of iterations was extended by 3000 and convergence was achieved after 4500 iterations in total, the first 3500 iterations were used as the burn-in period and the last 1000 iterations were used as the sampling period. With this procedure, when convergence was achieved for all parameters, the iterations were completed, and the last 1000 samples were adopted for estimation of the posterior distribution.

Tables 5 and 6 summarize the posterior mean and standard deviation of the regression coefficients and parameters (γ, ϕ, σ) for the trade price and trade volume. The estimation results for each date describe the results of the best model selected by DIC. Additionally, Figures 1 and 2 show the seasonality of trading interval durations estimated by the Bernstein polynomial. Since the regression coefficients of the Bernstein polynomial themselves do not have implications to be interpreted, the posterior statistics are presented as figures rather than tables of posterior statistics. The estimation results for each date describe the results of the best model selected by DIC. The DIC values for each model are summarized in Tables 5 and 6.

Then, let us discuss the posterior distribution in Tables 5 to 6.

Log return: β_1

In both March and April, the regression coefficients were not significant on all days. The results indicate that a short-term impact between trading intervals and returns was not observed. This is consistent with the results of Toyabe et al. (2024), in which the relationship between trading intervals and returns was examined in the stock market. In this respect, it can be said that the Bitcoin market has similar characteristics to conventional financial assets such as stocks. In addition, this result suggest that the relationship between trading intervals and volatility is not completely one-sided.

Price increase dummy: β_2

The posterior means were all positive for both March and April, and the results were statistically significant except for March 20th. The results indicate that when the trading price increases, the trading interval duration becomes longer than when the trading price does not change. Intuitively, we would expect the trading interval duration to be shorter when the price is increasing, as the market is considered to be more active. However, in reality, the trading interval duration was shorter when the price did not change.

Price decrease dummy: β_3

The posterior means were statistically significantly positive with the exception of March 20th. While β_2 is the effect of price increases, β_3 is the effect of price decreases on trade intervals.

Comparing the sizes of the posterior means, we found that there was no clear difference in the magnitude of β_2 and β_3. Therefore, both price increases and decreases have the similar effect of lengthening the duration of trades compared to when prices remain unchanged. In addition, March 20th was the only day when β_2 was not significant, so the Bitcoin market on that day is thought to have shown unusual patterns.

Trade volume: β_4

Both March and April's posterior means were a mixture of positive and negative signs, and they also contained both statistically significant and insignificant values. Even if considering only the significant values, their signs were a mixture of positive and negative signs. Therefore, we found that the impact of trading volume on trading interval duration differs depending on market conditions.

Price increase dummy × Trade volume: β_5

This is the effect of the trading volume on the trading interval duration. The regression coefficients were nearly all positive, and 25 out of 31 days in March and 21 out of 30 days in April were significant. This shows that when the price rises in response to a trade, the trading interval duration tends to increase in line with the trading volume.

Price increase dummy × Trade volume: β_6

In contrast to β_5, this is the effect of the trading volume on the trading interval duration when the price moves in the negative direction. The regression coefficients were generally negative and significant. This indicates that when the price decreases due to a trade, the trading duration tends to become shorter as opposed to β_5. This is similar to the leverage effect described in Section 1. Therefore, the Bitcoin market may also have a leverage effect in the same way as the stock markets.

Absolute log return × Trade volume: β_7

Looking at the posterior mean, although there were many negative values, they were mixed with positive values, and furthermore, they were not statistically significant on all days. Since this regression coefficient can be interpreted as the absolute impact of a trade on the market, we found that the impact of each trade does not affect the trading interval duration.

Shape parameter: γ

This parameter is related to the shape of the error term ϵ. The values were generally close to $\gamma = 1$ for all days in both March and April. When $\gamma \leq 1$, the mode of the Weibull distribution was zero; and when $\gamma > 1$, the mode was $\left(\frac{\gamma-1}{\gamma}\right)^{\frac{1}{\gamma}}$. In our setup, the mean and variance were calculated by using the gamma function $\Gamma(\cdot)$ as $\Gamma(1+\frac{1}{\gamma})$ and $\Gamma\left(1+\frac{2}{\gamma}\right)-\left(\Gamma\left(1+\frac{1}{\gamma}\right)\right)^2$. When $\gamma = 1$, both the mean and variance were 1.

AR(1) coefficient: ϕ

The minimum and maximum posterior means of ϕ in March and April were $(0.747, 0.946)$ and $(0, 705, 0.912)$, respectively. These results indicate that the trading interval duration for Bitcoin was strongly persistent. This result is consistent with that of Nakakita and Nakatsuma (2021), who conducted a volatility analysis using stock index data, and Toyabe and Nakatsuma (2022), who conducted a duration analysis using individual stock data. Thus, the Bitcoin market appears to have characteristics similar to those of the stock market.

Variance: σ^2

This parameter determines the variance of the AR(1) coefficient ϕ. Note that Tables 5 and 6 present σ instead of σ^2, but the latter was generally found to converge to a value close to 1.

The figures do not indicate any commonality in the intraday seasonality, nor was there any uniformity in the order of dimensions chosen. Based on these findings, it is likely that Bitcoin does not have a common seasonality for each day. This may be because the Bitcoin market has no restrictions on trading hours. The inverse U-shaped seasonality observed by Toyabe and Nakatsuma (2022) can be attributed to the fact that the market for the analyzed financial instruments had opening and closing times, so there was a rush of orders immediately after the market opened and just before it closed. The Bitcoin market is open 24 hours a day, so time is not a factor when making orders. However, we extracted data only during the trading hours of the US stock market to examine its relationship with the Bitcoin market. Because we could not identify any seasonality common to all days, we found no clear relationship between the trading interval durations of the Bitcoin market and US stock market. In addition, there were no major differences from day to day, and no clear differences were observed between weekdays and weekends. As a result, whether the stock market was open or closed made no impact on the trade interval durations of the Bitcoin market.

Table 3. DIC values of models with different orders of Bernstein polynomials (March 2024).

	4	8	12	16
2024-03-01	-9.0496×10^6	$\mathbf{-9.0576 \times 10^6}$	-9.0356×10^6	-9.0018×10^6
2024-03-02	$\mathbf{-7.2145 \times 10^6}$	-7.1812×10^6	-7.1501×10^6	-7.0949×10^6
2024-03-03	$\mathbf{-8.8674 \times 10^6}$	-8.7836×10^6	-8.7488×10^6	-8.7215×10^6
2024-03-04	-1.3502×10^7	-1.3515×10^7	$\mathbf{-1.3517 \times 10^7}$	-1.3513×10^7
2024-03-05	$\mathbf{-1.5343 \times 10^7}$	-1.5325×10^7	-1.5333×10^7	-1.5321×10^7
2024-03-06	-1.5249×10^7	-1.5297×10^7	-1.5321×10^7	$\mathbf{-1.5365 \times 10^7}$
2024-03-07	$\mathbf{-1.0135 \times 10^7}$	-1.0086×10^7	-1.0077×10^7	-1.0065×10^7
2024-03-08	$\mathbf{-1.3809 \times 10^7}$	-1.3783×10^7	-1.3752×10^7	-1.3742×10^7
2024-03-09	$\mathbf{-5.6867 \times 10^6}$	-5.6852×10^6	-5.6783×10^6	-5.6728×10^6
2024-03-10	-9.8849×10^6	$\mathbf{-9.8904 \times 10^6}$	-9.8835×10^6	$-9,8797 \times 10^6$
2024-03-11	-1.4258×10^7	-1.4270×10^7	$\mathbf{-1.4279 \times 10^7}$	-1.4269×10^7
2024-03-12	-1.2099×10^7	-1.2120×10^7	-1.2151×10^7	$\mathbf{-1.2162 \times 10^7}$
2024-03-13	-1.0929×10^7	-1.0939×10^7	$\mathbf{-1.0945 \times 10^7}$	-1.0941×10^7
2024-03-14	-1.1017×10^7	$\mathbf{-1.1042 \times 10^7}$	-1.1032×10^7	-1.1034×10^7
2024-03-15	-1.1950×10^7	-1.1967×10^7	-1.1981×10^7	$\mathbf{-1.1986 \times 10^7}$
2024-03-16	-9.9812×10^6	-1.0005×10^7	-9.9992×10^6	$\mathbf{-1.0013 \times 10^7}$
2024-03-17	-8.0717×10^6	-8.0887×10^6	-8.0957×10^6	$\mathbf{-8.1017 \times 10^6}$
2024-03-18	-8.7707×10^6	-8.7824×10^6	-8.7894×10^6	$\mathbf{-8.7937 \times 10^6}$
2024-03-19	-1.4068×10^7	-1.4191×10^7	-1.4248×10^6	$\mathbf{-1.4284 \times 10^6}$
2024-03-20	-1.1701×10^7	-1.1703×10^7	$\mathbf{-1.1703 \times 10^7}$	-1.1703×10^7
2024-03-21	-6.9164×10^6	-6.9307×10^6	-6.9343×10^6	$\mathbf{-6.9385 \times 10^6}$
2024-03-22	-1.0496×10^7	-1.0521×10^7	-1.0542×10^7	$\mathbf{-1.0549 \times 10^7}$
2024-03-23	-5.5519×10^6	-5.5637×10^6	$\mathbf{-5.5700 \times 10^6}$	-5.5646×10^6
2024-03-24	-5.3719×10^6	-5.3973×10^6	$\mathbf{-5.4061 \times 10^6}$	-5.3985×10^6
2024-03-25	-1.0146×10^7	-1.0138×10^7	-1.0135×10^7	$\mathbf{-1.0144 \times 10^7}$
2024-03-26	-8.9503×10^6	-8.9509×10^6	$\mathbf{-8.9541 \times 10^6}$	-8.9524×10^6
2024-03-27	-1.2709×10^7	-1.2735×10^7	-1.2751×10^7	$\mathbf{-1.2758 \times 10^7}$
2024-03-28	-8.1373×10^6	$\mathbf{-8.1503 \times 10^6}$	-8.1492×10^6	-8.1489×10^6
2024-03-29	-5.8772×10^6	$\mathbf{-5.8788 \times 10^6}$	-5.8735×10^6	-5.8704×10^6
2024-03-30	$\mathbf{-3.8046 \times 10^6}$	-3.7943×10^6	-3.7777×10^6	-3.7634×10^6
2024-03-31	$\mathbf{-4.4657 \times 10^6}$	-4.4571×10^6	-4.4402×10^6	-4.4115×10^6

Table 4. DIC values of models with different orders of Bernstein polynomials (April 2024).

	4	8	12	16
2024-04-01	-6.5504×10^6	$\mathbf{-6.5526 \times 10^6}$	-6.5509×10^6	-6.5421×10^6
2024-04-02	-1.0156×10^7	-1.0160×10^7	-1.0166×10^7	$\mathbf{-1.0173 \times 10^7}$
2024-04-03	$\mathbf{-6.8556 \times 10^6}$	-6.8539×10^6	-6.8547×10^6	-6.8455×10^6
2024-04-04	-6.9519×10^6	-6.9552×10^6	$\mathbf{-6.9572 \times 10^6}$	-6.9562×10^6
2024-04-05	-8.0626×10^6	-8.0850×10^6	-8.0908×10^6	$\mathbf{-8.0942 \times 10^6}$
2024-04-06	$\mathbf{-4.7878 \times 10^6}$	-4.7736×10^6	-4.7615×10^6	-4.7362×10^6
2024-04-07	-3.9501×10^6	$\mathbf{-3.9571 \times 10^6}$	-3.9523×10^6	-3.9399×10^6
2024-04-08	-1.1823×10^7	-1.1854×10^7	-1.1863×10^7	$\mathbf{-1.1875 \times 10^7}$
2024-04-09	-7.7884×10^6	-7.7856×10^6	-7.7905×10^6	$\mathbf{-7.7936 \times 10^6}$
2024-04-10	-8.1812×10^6	-8.1832×10^6	-8.1832×10^6	$\mathbf{-8.1852 \times 10^6}$
2024-04-11	-8.9400×10^6	-9.0063×10^6	-9.0446×10^6	$\mathbf{-9.0644 \times 10^6}$
2024-04-12	-9.4738×10^6	-9.5479×10^6	-9.5991×10^6	$\mathbf{-9.6012 \times 10^6}$
2024-04-13	-5.1372×10^6	-5.1446×10^6	$\mathbf{-5.1462 \times 10^6}$	-5.1386×10^6
2024-04-14	-7.7846×10^6	-7.8298×10^6	-7.8494×10^6	$\mathbf{-7.8680 \times 10^6}$
2024-04-15	-8.6526×10^6	-8.6815×10^6	-8.7106×10^6	$\mathbf{-8.7296 \times 10^6}$
2024-04-16	-1.3220×10^7	-1.3326×10^7	-1.3500×10^7	$\mathbf{-1.3564 \times 10^7}$
2024-04-17	-1.1961×10^7	-1.2037×10^7	-1.2103×10^7	$\mathbf{-1.2104 \times 10^7}$
2024-04-18	-1.0244×10^7	-1.0280×10^7	-1.0316×10^7	$\mathbf{-1.0323 \times 10^7}$
2024-04-19	-8.4024×10^6	-8.4457×10^6	-8.4902×10^6	$\mathbf{-8.5086 \times 10^6}$
2024-04-20	-4.3427×10^6	-4.3459×10^6	$\mathbf{-4.3491 \times 10^6}$	-4.3439×10^6
2024-04-21	-4.5195×10^6	$\mathbf{-4.5370 \times 10^6}$	-4.5261×10^6	-4.5186×10^6
2024-04-22	-5.4320×10^6	-5.4689×10^6	-5.4781×10^6	$\mathbf{-5.4809 \times 10^6}$
2024-04-23	-6.7993×10^6	-6.8654×10^6	$\mathbf{-6.8663 \times 10^6}$	-6.8644×10^6
2024-04-24	-7.7319×10^6	-7.7457×10^6	$\mathbf{-7.7484 \times 10^6}$	-7.7444×10^6
2024-04-25	-6.5406×10^6	-6.5604×10^6	-6.5929×10^6	$\mathbf{-6.6185 \times 10^6}$
2024-04-26	-5.1815×10^6	-5.1954×10^6	$\mathbf{-5.2050 \times 10^6}$	-5.2015×10^6
2024-04-27	$\mathbf{-3.0679 \times 10^6}$	-3.0611×10^6	-3.0531×10^6	-3.0492×10^6
2024-04-28	$\mathbf{-2.7065 \times 10^6}$	-2.7047×10^6	-2.6996×10^6	-2.6940×10^6
2024-04-29	-4.6556×10^6	-4.6736×10^6	$\mathbf{-4.6823 \times 10^6}$	-4.6799×10^6
2024-04-30	-8.8502×10^6	-8.8767×10^6	-8.9027×10^6	$\mathbf{-8.9120 \times 10^6}$

Table 5. Estimation results of the best model selected by DIC (March 2024).

Date	β_1	β_2	β_3	β_4	β_5	β_6	β_7	γ	ϕ	σ
2024-03-01	7.501×10^{-2}	$\mathbf{2.154 \times 10^{-1}}$	$\mathbf{2.234 \times 10^{-1}}$	-1.367×10^{-2}	$\mathbf{2.756 \times 10^{-1}}$	$\mathbf{-1.879 \times 10^{-1}}$	-1.186×10^{-1}	1.131	0.929	0.688
	(9.839×10^{-1})	(8.311×10^{-3})	(8.564×10^{-3})	(2.104×10^{-2})	(2.580×10^{-2})	(2.501×10^{-2})	(1.000×10^{0})	(4.434×10^{-3})	(1.065×10^{-3})	(3.605×10^{-3})
2024-03-02	1.060×10^{-2}	$\mathbf{1.542 \times 10^{-1}}$	$\mathbf{1.781 \times 10^{-1}}$	4.850×10^{-2}	$\mathbf{1.930 \times 10^{-1}}$	$\mathbf{-2.552 \times 10^{-1}}$	-7.272×10^{-2}	1.109	0.946	0.638
	(9.944×10^{-1})	(9.729×10^{-3})	(9.215×10^{-3})	(3.029×10^{-2})	(3.618×10^{-2})	(3.702×10^{-2})	(9.988×10^{-1})	(3.987×10^{-3})	(9.257×10^{-4})	(3.691×10^{-3})
2024-03-03	8.456×10^{-3}	$\mathbf{1.918 \times 10^{-1}}$	$\mathbf{2.280 \times 10^{-1}}$	$\mathbf{6.134 \times 10^{-2}}$	2.372×10^{-2}	$\mathbf{-2.350 \times 10^{-1}}$	-3.785×10^{-2}	1.130	0.936	0.663
	(1.000×10^{0})	(1.273×10^{-2})	(1.199×10^{-2})	(2.865×10^{-2})	(3.196×10^{-2})	(3.362×10^{-2})	(9.997×10^{-1})	(4.432×10^{-3})	(1.156×10^{-3})	(4.056×10^{-3})
2024-03-04	-1.886×10^{-2}	$\mathbf{2.189 \times 10^{-1}}$	$\mathbf{2.186 \times 10^{-1}}$	-1.034×10^{-2}	$\mathbf{5.907 \times 10^{-2}}$	$\mathbf{-4.828 \times 10^{-2}}$	-2.516×10^{-1}	1.111	0.914	0.623
	(9.805×10^{-1})	(6.549×10^{-3})	(6.398×10^{-3})	(1.360×10^{-2})	(1.655×10^{-2})	(1.660×10^{-2})	(9.960×10^{-1})	(3.039×10^{-3})	(1.006×10^{-3})	(2.740×10^{-3})
2024-03-05	-3.660×10^{-2}	$\mathbf{2.168 \times 10^{-1}}$	$\mathbf{2.233 \times 10^{-1}}$	1.617×10^{-2}	1.604×10^{-2}	$\mathbf{-8.226 \times 10^{-2}}$	6.022×10^{-1}	1.121	0.910	0.601
	(1.040)	(6.243×10^{-3})	(6.571×10^{-3})	(1.492×10^{-2})	(1.613×10^{-2})	(1.693×10^{-2})	(9.710×10^{-1})	(3.362×10^{-3})	(1.076×10^{-3})	(2.579×10^{-3})
2024-03-06	8.772×10^{-2}	$\mathbf{2.653 \times 10^{-1}}$	$\mathbf{2.565 \times 10^{-1}}$	-2.094×10^{-2}	$\mathbf{1.711 \times 10^{-1}}$	$\mathbf{-1.239 \times 10^{-1}}$	-4.981×10^{-1}	1.160	0.811	0.841
	(9.989×10^{-1})	(5.659×10^{-3})	(6.253×10^{-3})	(2.000×10^{-2})	(2.276×10^{-2})	(2.147×10^{-2})	(1.020)	(4.768×10^{-3})	(2.301×10^{-3})	(4.763×10^{-3})
2024-03-07	2.079×10^{-2}	$\mathbf{2.160 \times 10^{-1}}$	$\mathbf{2.172 \times 10^{-1}}$	-9.789×10^{-3}	$\mathbf{6.201 \times 10^{-2}}$	$\mathbf{-1.798 \times 10^{-1}}$	-1.238×10^{-1}	1.867	0.916	0.678
	(1.016)	(8.643×10^{-3})	(9.304×10^{-3})	(1.958×10^{-2})	(2.105×10^{-2})	(2.225×10^{-2})	(9.730×10^{-1})	(3.592×10^{-3})	(1.255×10^{-3})	(3.063×10^{-3})
2024-03-08	-1.791×10^{-2}	$\mathbf{1.854 \times 10^{-1}}$	$\mathbf{1.879 \times 10^{-1}}$	-4.910×10^{-3}	$\mathbf{1.019 \times 10^{-1}}$	$\mathbf{-7.669 \times 10^{-2}}$	-2.275×10^{-1}	1.106	0.928	0.504
	(1.002)	(6.704×10^{-3})	(6.901×10^{-3})	(6.878×10^{-3})	(1.013×10^{-2})	(9.291×10^{-3})	(9.841×10^{-1})	(2.857×10^{-3})	(1.025×10^{-3})	(2.512×10^{-3})
2024-03-09	-1.814×10^{-3}	$\mathbf{2.132 \times 10^{-1}}$	$\mathbf{2.130 \times 10^{-1}}$	-7.701×10^{-2}	$\mathbf{4.316 \times 10^{-1}}$	$\mathbf{-3.068 \times 10^{-1}}$	2.964×10^{-2}	0.967	0.936	0.552
	(9.968×10^{-1})	(8.169×10^{-3})	(8.403×10^{-3})	(4.149×10^{-2})	(5.298×10^{-2})	(5.384×10^{-2})	(9.943×10^{-1})	(2.962×10^{-3})	(1.030×10^{-3})	(3.213×10^{-3})
2024-03-10	1.068×10^{-2}	$\mathbf{2.159 \times 10^{-1}}$	$\mathbf{2.228 \times 10^{-1}}$	3.545×10^{-2}	$\mathbf{7.673 \times 10^{-2}}$	$\mathbf{-1.479 \times 10^{-1}}$	-2.956×10^{-1}	1.069	0.919	0.645
	(9.618×10^{-1})	(7.715×10^{-3})	(7.733×10^{-3})	(1.912×10^{-2})	(2.591×10^{-2})	(2.246×10^{-2})	(9.892×10^{-1})	(3.459×10^{-3})	(1.213×10^{-3})	(4.158×10^{-3})
2024-03-11	7.079×10^{-2}	$\mathbf{2.214 \times 10^{-1}}$	$\mathbf{2.136 \times 10^{-1}}$	1.230×10^{-3}	$\mathbf{1.594 \times 10^{-1}}$	$\mathbf{-1.191 \times 10^{-1}}$	5.466×10^{-2}	1.110	0.893	0.626
	(9.833×10^{-1})	(5.848×10^{-3})	(5.966×10^{-3})	(9.561×10^{-3})	(1.423×10^{-2})	(1.307×10^{-2})	(1.006)	(2.995×10^{-3})	(1.444×10^{-3})	(3.304×10^{-3})
2024-03-12	1.393×10^{-3}	$\mathbf{2.854 \times 10^{-1}}$	$\mathbf{2.815 \times 10^{-1}}$	$\mathbf{3.730 \times 10^{-2}}$	$\mathbf{1.104 \times 10^{-1}}$	$\mathbf{-1.891 \times 10^{-1}}$	-5.393×10^{-1}	1.118	0.885	0.729
	(1.005)	(6.362×10^{-3})	(6.357×10^{-3})	(1.822×10^{-2})	$2.183 \times 10^{-2})$	(2.231×10^{-2})	(9.989×10^{-1})	(3.575×10^{-3})	(1.444×10^{-3})	(3.370×10^{-3})
2024-03-13	-2.336×10^{-2}	$\mathbf{1.851 \times 10^{-1}}$	$\mathbf{1.705 \times 10^{-1}}$	-1.700×10^{-2}	$\mathbf{2.474 \times 10^{-1}}$	$\mathbf{-1.392 \times 10^{-1}}$	-5.603×10^{-2}	1.065	0.920	0.582
	(9.906×10^{-1})	(6.365×10^{-3})	(6.478×10^{-3})	(1.706×10^{-2})	(2.284×10^{-2})	(2.014×10^{-2})	(9.939×10^{-1})	(2.722×10^{-3})	(1.028×10^{-3})	(2.834×10^{-3})
2024-03-14	3.088×10^{-2}	$\mathbf{2.446 \times 10^{-1}}$	$\mathbf{2.366 \times 10^{-1}}$	-1.407×10^{-3}	$\mathbf{2.177 \times 10^{-1}}$	$\mathbf{-1.186 \times 10^{-1}}$	4.148×10^{-1}	1.065	0.871	0.688
	(9.986×10^{-1})	(6.520×10^{-3})	(6.296×10^{-3})	(2.010×10^{-2})	(2.365×10^{-2})	(2.195×10^{-2})	(9.974×10^{-1})	(3.637×10^{-3})	(1.703×10^{-3})	(4.022×10^{-3})
2024-03-15	1.267×10^{-2}	$\mathbf{2.098 \times 10^{-1}}$	$\mathbf{2.037 \times 10^{-1}}$	5.815×10^{-3}	$\mathbf{1.526 \times 10^{-1}}$	$\mathbf{-2.565 \times 10^{-1}}$	1.163×10^{-1}	1.086	0.830	0.741
	(9.747×10^{-1})	(5.850×10^{-3})	(5.839×10^{-3})	(2.021×10^{-2})	(2.289×10^{-2})	(2.243×10^{-2})	(9.703×10^{-1})	(3.048×10^{-3})	(1.723×10^{-3})	(3.443×10^{-3})

The upper number is the posterior mean, and the lower number in parentheses is the posterior standard deviation.
The boldface in the posterior mean indicates that $\boldsymbol{\beta}$ does not include a zero in the 95% credible interval.

Table 5. Estimation results of the best model selected by DIC (March 2024) (continued).

Date	β_1	β_2	β_3	β_4	β_5	β_6	β_7	γ	ϕ	σ
2024-03-16	-2.145×10^{-2}	**2.742×10^{-1}**	**2.668×10^{-1}**	1.892×10^{-2}	**2.489×10^{-1}**	**-2.040×10^{-1}**	-5.631×10^{-3}	1.105	0.900	0.714
	(9.962×10^{-1})	(8.695×10^{-3})	(8.466×10^{-3})	(2.646×10^{-2})	(3.270×10^{-2})	(2.873×10^{-2})	(1.023)	(3.452×10^{-3})	(1.309×10^{-3})	(3.750×10^{-3})
2024-03-17	4.001×10^{-2}	**2.678×10^{-1}**	**2.738×10^{-1}**	2.255×10^{-2}	**1.462×10^{-1}**	**-3.908×10^{-1}**	3.684×10^{-1}	1.055	8.424	0.791
	(9.853×10^{-1})	(7.155×10^{-3})	(7.130×10^{-3})	(2.975×10^{-2})	(3.195×10^{-2})	(3.464×10^{-2})	(1.002)	(5.333×10^{-3})	(2.771×10^{-3})	(7.974×10^{-3})
2024-03-18	-2.987×10^{-2}	**2.615×10^{-1}**	**2.597×10^{-1}**	5.977×10^{-3}	**2.514×10^{-1}**	**-2.688×10^{-1}**	1.095×10^{-2}	1.049	0.852	0.773
	(9.744×10^{-1})	(7.321×10^{-3})	(6.822×10^{-3})	(2.946×10^{-2})	(3.234×10^{-2})	(3.144×10^{-2})	(9.688×10^{-1})	(4.567×10^{-3})	(2.066×10^{-3})	(5.701×10^{-3})
2024-03-19	2.536×10^{-2}	**3.563×10^{-1}**	**3.532×10^{-1}**	**3.429×10^{-2}**	**1.253×10^{-1}**	**-2.599×10^{-1}**	-4.439×10^{-1}	1.160	0.747	0.950
	(9.998×10^{-1})	(6.157×10^{-3})	(5.912×10^{-3})	(1.543×10^{-2})	(1.791×10^{-2})	(1.861×10^{-2})	(1.006)	(5.468×10^{-3})	(2.394×10^{-3})	(4.456×10^{-3})
2024-03-20	5.092×10^{-2}	3.567×10^{-3}	**-2.643×10^{-2}**	1.207×10^{-3}	**1.941×10^{-1}**	**-1.459×10^{-1}**	2.470×10^{-2}	1.049	0.861	0.602
	(9.879×10^{-1})	(5.255×10^{-3})	(5.168×10^{-3})	(2.426×10^{-2})	(2.594×10^{-2})	(2.626×10^{-2})	(9.590×10^{-1})	(2.773×10^{-3})	(1.572×10^{-3})	(3.684×10^{-3})
2024-03-21	3.553×10^{-2}	**1.344×10^{-1}**	**1.245×10^{-1}**	**1.397×10^{-1}**	**8.008×10^{-2}**	**-3.630×10^{-1}**	-7.269×10^{-1}	1.034	0.826	0.848
	(9.689×10^{-1})	(7.847×10^{-3})	(8.425×10^{-3})	(3.460×10^{-2})	(3.750×10^{-2})	(3.776×10^{-2})	(9.654×10^{-1})	(4.339×10^{-3})	(2.187×10^{-3})	(4.902×10^{-3})
2024-03-22	2.581×10^{-2}	**2.746×10^{-1}**	**2.699×10^{-1}**	**-7.148×10^{-2}**	**3.143×10^{-1}**	**-1.182×10^{-1}**	-2.092×10^{-1}	1.082	0.801	0.873
	(9.730×10^{-1})	(6.301×10^{-3})	(6.493×10^{-3})	(2.344×10^{-2})	(2.642×10^{-2})	(2.596×10^{-2})	(1.002)	(3.853×10^{-3})	(1.784×10^{-3})	(3.863×10^{-3})
2024-03-23	1.314×10^{-3}	**2.254×10^{-1}**	**2.271×10^{-1}**	-2.507×10^{-2}	**2.322×10^{-1}**	**-1.429×10^{-1}**	-4.210×10^{-2}	1.021	0.861	0.902
	(9.633×10^{-1})	(9.369×10^{-3})	(9.782×10^{-3})	(3.913×10^{-2})	(4.344×10^{-2})	(4.547×10^{-2})	(9.884×10^{-1})	(4.734×10^{-3})	(2.055×10^{-3})	(5.211×10^{-3})
2024-03-24	2.684×10^{-2}	**2.095×10^{-1}**	**2.344×10^{-1}**	-2.441×10^{-2}	**1.038×10^{-1}**	**-2.423×10^{-1}**	-8.933×10^{-2}	1.066	0.863	0.982
	(9.917×10^{-1})	(1.215×10^{-2})	(1.227×10^{-2})	(3.068×10^{-2})	(3.357×10^{-2})	(4.109×10^{-2})	(9.883×10^{-1})	(6.032×10^{-3})	(2.100×10^{-3})	(6.052×10^{-3})
2024-03-25	-1.956×10^{-3}	**3.015×10^{-1}**	**2.042×10^{-1}**	**1.321×10^{-1}**	-1.640×10^{-2}	**-2.206×10^{-1}**	5.264×10^{-1}	1.100	0.812	0.872
	(1.013)	(7.148×10^{-3})	(6.912×10^{-3})	(1.937×10^{-2})	(2.114×10^{-2})	(2.104×10^{-2})	(1.009)	(4.718×10^{-3})	(2.214×10^{-3})	(4.164×10^{-3})
2024-03-26	-4.923×10^{-3}	**2.364×10^{-1}**	**1.677×10^{-2}**	**6.872×10^{-2}**	**8.344×10^{-2}**	**-2.181×10^{-1}**	-5.847×10^{-2}	1.021	0.865	0.752
	(1.010)	(6.981×10^{-3})	(7.179×10^{-3})	(2.378×10^{-2})	(2.665×10^{-2})	(2.707×10^{-2})	(9.794×10^{-1})	(3.135×10^{-3})	(1.412×10^{-3})	(3.234×10^{-3})
2024-03-27	2.732×10^{-2}	**3.194×10^{-1}**	**3.328×10^{-1}**	-1.617×10^{-2}	**1.013×10^{-1}**	**-7.794×10^{-2}**	7.406×10^{-1}	1.122	0.846	0.805
	(1.022)	(7.706×10^{-3})	(7.544×10^{-3})	(2.047×10^{-2})	(2.244×10^{-2})	(2.267×10^{-2})	(9.992×10^{-1})	(6.010×10^{-3})	(2.407×10^{-3})	(6.190×10^{-3})
2024-03-28	3.788×10^{-2}	**2.292×10^{-1}**	**2.117×10^{-1}**	-1.276×10^{-2}	5.266×10^{-2}	**-1.147×10^{-1}**	-2.313×10^{-1}	1.033	0.873	0.731
	(9.649×10^{-1})	(7.810×10^{-3})	(7.641×10^{-3})	(2.531×10^{-2})	(2.646×10^{-2})	(2.810×10^{-2})	(1.026)	(3.882×10^{-3})	(1.745×10^{-3})	(3.978×10^{-3})
2024-03-29	-2.574×10^{-2}	**1.586×10^{-1}**	**1.248×10^{-1}**	**-1.056×10^{-1}**	**4.290×10^{-1}**	2.296×10^{-2}	-2.591×10^{-1}	0.998	0.898	0.732
	(9.720×10^{-1})	(9.144×10^{-3})	(8.984×10^{-3})	(3.051×10^{-2})	(3.798×10^{-2})	(3.285×10^{-2})	(1.030)	(3.889×10^{-3})	(1.578×10^{-3})	(4.537×10^{-3})
2024-03-30	-2.030×10^{-2}	**1.464×10^{-1}**	**1.359×10^{-1}**	6.014×10^{-2}	1.258×10^{-1}	-1.298×10^{-1}	-8.932×10^{-2}	1.040	0.934	0.681
	(9.899×10^{-1})	(9.987×10^{-3})	(1.022×10^{-2})	(6.259×10^{-2})	(6.966×10^{-2})	(7.159×10^{-2})	(1.025)	(4.364×10^{-3})	(1.165×10^{-3})	(3.654×10^{-3})
2024-03-31	-1.184×10^{-2}	**1.399×10^{-1}**	**1.595×10^{-1}**	2.228×10^{-3}	**1.092×10^{-1}**	**-1.989×10^{-1}**	-6.649×10^{-2}	1.059	0.934	0.718
	(9.640×10^{-1})	(1.369×10^{-2})	(1.364×10^{-2})	(3.569×10^{-2})	(4.321×10^{-2})	(4.232×10^{-2})	(1.014)	(4.552×10^{-3})	(1.200×10^{-3})	(3.255×10^{-3})

The upper number is the posterior mean, and the lower number in parentheses is the posterior standard deviation.
The boldface in the posterior mean indicates that $\boldsymbol{\beta}$ does not include a zero in the 95% credible interval.

Table 6. Estimation results of the best model selected by DIC (April 2024).

Date	β_1	β_2	β_3	β_4	β_5	β_6	β_7	γ	ϕ	σ
2024-04-01	1.816×10^{-3}	$\mathbf{2.626 \times 10^{-1}}$	$\mathbf{2.126 \times 10^{-1}}$	1.366×10^{-2}	$\mathbf{2.882 \times 10^{-1}}$	$\mathbf{-1.685 \times 10^{-1}}$	-1.017×10^{-1}	1.040	0.878	0.780
	(1.010)	(9.016×10^{-3})	(9.719×10^{-3})	(2.690×10^{-2})	$3.384 \times 10^{-2})$	(2.983×10^{-2})	(9.712×10^{-1})	(4.861×10^{-3})	(2.000×10^{-3})	(6.102×10^{-3})
2024-04-02	4.952×10^{-2}	$\mathbf{1.642 \times 10^{-1}}$	$\mathbf{1.431 \times 10^{-1}}$	$\mathbf{-3.473 \times 10^{-2}}$	$\mathbf{8.477 \times 10^{-2}}$	$\mathbf{3.769 \times 10^{-2}}$	-6.585×10^{-1}	1.019	0.872	0.660
	(9.680×10^{-1})	(6.553×10^{-3})	(6.714×10^{-3})	(1.366×10^{-2})	$1.472 \times 10^{-2})$	(1.526×10^{-2})	(1.011)	(3.217×10^{-3})	(1.772×10^{-3})	(4.771×10^{-3})
2024-04-03	6.340×10^{-2}	$\mathbf{1.235 \times 10^{-1}}$	$\mathbf{7.310 \times 10^{-2}}$	3.566×10^{-2}	5.546×10^{-2}	$\mathbf{-1.453 \times 10^{-1}}$	-4.442×10^{-2}	0.989	0.912	0.642
	(1.014)	(7.833×10^{-3})	(7.407×10^{-3})	(3.184×10^{-2})	(3.402×10^{-2})	(3.500×10^{-2})	(9.899×10^{-1})	(3.428×10^{-3})	(1.370×10^{-3})	(3.580×10^{-3})
2024-04-04	1.926×10^{-2}	$\mathbf{1.689 \times 10^{-1}}$	$\mathbf{1.227 \times 10^{-1}}$	-1.413×10^{-2}	3.254×10^{-2}	-2.729×10^{-2}	-2.416×10^{-1}	1.043	0.886	0.730
	(1.013)	(7.896×10^{-3})	(8.024×10^{-3})	(2.262×10^{-2})	(2.484×10^{-2})	(2.570×10^{-2})	(1.001)	(3.864×10^{-3})	(1.578×10^{-3})	(4.703×10^{-3})
2024-04-05	1.370×10^{-1}	$\mathbf{2.420 \times 10^{-1}}$	$\mathbf{2.304 \times 10^{-1}}$	2.497×10^{-2}	4.781×10^{-2}	$\mathbf{-9.778 \times 10^{-2}}$	2.665×10^{-1}	1.063	0.852	0.853
	(1.023)	(8.156×10^{-3})	(8.325×10^{-3})	(2.817×10^{-2})	(2.936×10^{-2})	(3.073×10^{-2})	(9.803×10^{-1})	(4.577×10^{-3})	(1.912×10^{-3})	(4.576×10^{-3})
2024-04-06	1.744×10^{-2}	$\mathbf{1.599 \times 10^{-1}}$	$\mathbf{1.413 \times 10^{-1}}$	-4.771×10^{-2}	5.744×10^{-2}	1.084×10^{-2}	-3.085×10^{-1}	1.087	0.928	0.710
	(1.021)	(1.290×10^{-2})	(1.300×10^{-2})	(3.274×10^{-2})	(3.596×10^{-2})	(3.873×10^{-2})	(1.027)	(5.123×10^{-3})	(1.414×10^{-3})	(4.612×10^{-3})
2024-04-07	4.870×10^{-3}	$\mathbf{2.132 \times 10^{-1}}$	$\mathbf{1.755 \times 10^{-1}}$	$\mathbf{1.374 \times 10^{-1}}$	9.043×10^{-2}	$\mathbf{-2.817 \times 10^{-1}}$	7.648×10^{-2}	1.053	0.889	0.864
	(9.876×10^{-1})	(1.109×10^{-2})	(1.086×10^{-2})	(4.509×10^{-2})	(5.160×10^{-2})	(5.397×10^{-2})	(9.766×10^{-1})	(6.293×10^{-3})	(1.909×10^{-3})	(6.625×10^{-3})
2024-04-08	7.711×10^{-2}	$\mathbf{2.859 \times 10^{-1}}$	$\mathbf{2.819 \times 10^{-1}}$	$\mathbf{1.712 \times 10^{-1}}$	$\mathbf{-9.462 \times 10^{-2}}$	$\mathbf{-3.320 \times 10^{-1}}$	-1.039×10^{-1}	1.141	0.835	0.833
	(1.010)	(6.403×10^{-3})	(6.657×10^{-3})	(2.296×10^{-2})	(2.543×10^{-2})	(2.754×10^{-2})	(9.678×10^{-1})	(5.574×10^{-3})	(2.128×10^{-3})	(5.528×10^{-3})
2024-04-09	9.347×10^{-2}	$\mathbf{3.421 \times 10^{-1}}$	$\mathbf{3.353 \times 10^{-1}}$	1.211×10^{-2}	$\mathbf{1.186 \times 10^{-1}}$	$\mathbf{-5.177 \times 10^{-2}}$	5.981×10^{-1}	1.055	0.835	0.882
	(9.966×10^{-1})	(8.261×10^{-3})	(8.215×10^{-3})	(2.215×10^{-2})	(2.557×10^{-2})	(2.489×10^{-2})	(9.893×10^{-1})	(4.842×10^{-3})	(2.342×10^{-3})	(6.011×10^{-3})
2024-04-10	8.800×10^{-3}	$\mathbf{2.656 \times 10^{-1}}$	$\mathbf{2.584 \times 10^{-1}}$	$\mathbf{-6.512 \times 10^{-2}}$	1.683×10^{-1}	-1.543×10^{-2}	-1.838×10^{-1}	1.087	0.844	0.871
	(1.013)	(8.028×10^{-3})	(8.018×10^{-3})	(1.874×10^{-2})	(2.292×10^{-2})	(2.214×10^{-2})	(9.288×10^{-1})	(4.495×10^{-3})	(1.848×10^{-3})	(4.531×10^{-3})
2024-04-11	-7.104×10^{-3}	$\mathbf{3.354 \times 10^{-1}}$	$\mathbf{3.290 \times 10^{-1}}$	$\mathbf{1.271 \times 10^{-1}}$	$\mathbf{-7.428 \times 10^{-2}}$	$\mathbf{-2.665 \times 10^{-1}}$	-1.831×10^{-1}	1.154	0.797	1.071
	(9.932×10^{-1})	(9.125×10^{-3})	(9.615×10^{-3})	(2.729×10^{-2})	(2.961×10^{-2})	(3.128×10^{-2})	(1.016)	(6.922×10^{-3})	(2.435×10^{-3})	(5.249×10^{-3})
2024-04-12	1.365×10^{-2}	$\mathbf{3.389 \times 10^{-1}}$	$\mathbf{3.324 \times 10^{-1}}$	1.058×10^{-2}	1.025×10^{-2}	$\mathbf{-1.430 \times 10^{-1}}$	-3.380×10^{-1}	1.176	0.860	0.955
	(1.004)	(1.022×10^{-2})	(9.669×10^{-3})	(2.048×10^{-2})	(2.240×10^{-2})	(2.404×10^{-2})	(9.825×10^{-1})	(6.149×10^{-3})	(1.602×10^{-3})	(3.777×10^{-3})
2024-04-13	-6.398×10^{-3}	$\mathbf{1.105 \times 10^{-1}}$	$\mathbf{1.543 \times 10^{-1}}$	4.012×10^{-2}	$\mathbf{1.364 \times 10^{-1}}$	$\mathbf{-1.557 \times 10^{-1}}$	4.070×10^{-2}	1.016	0.901	0.778
	(1.009)	(8.983×10^{-3})	(9.413×10^{-3})	(5.228×10^{-2})	(5.506×10^{-2})	(4.531×10^{-2})	(9.866×10^{-1})	(4.102×10^{-3})	(1.412×10^{-3})	(4.175×10^{-3})
2024-04-14	8.563×10^{-2}	$\mathbf{1.859 \times 10^{-1}}$	$\mathbf{1.930 \times 10^{-1}}$	4.718×10^{-2}	$\mathbf{1.395 \times 10^{-1}}$	$\mathbf{-1.040 \times 10^{-1}}$	-9.262×10^{-1}	1.092	0.805	1.029
	(9.887×10^{-1})	(8.584×10^{-3})	(9.208×10^{-3})	(2.442×10^{-2})	(2.852×10^{-2})	(2.586×10^{-2})	(1.007)	(6.767×10^{-3})	(2.580×10^{-3})	(6.897×10^{-3})
2024-04-15	3.427×10^{-2}	$\mathbf{2.246 \times 10^{-1}}$	$\mathbf{2.265 \times 10^{-1}}$	1.816×10^{-2}	$\mathbf{1.622 \times 10^{-1}}$	$\mathbf{-8.644 \times 10^{-2}}$	4.503×10^{-1}	1.123	0.797	1.016
	(9.848×10^{-1})	(8.663×10^{-3})	(8.832×10^{-3})	(2.446×10^{-2})	(3.029×10^{-2})	(2.629×10^{-2})	(1.018)	(5.854×10^{-3})	(2.323×10^{-3})	(4.856×10^{-3})

The upper number is the posterior mean, and the lower number in parentheses is the posterior standard deviation.
The boldface in the posterior mean indicates that $\boldsymbol{\beta}$ does not include a zero in the 95% credible interval.

Table 6. Estimation results of the best model selected by DIC (April 2024) (continued).

Date	β_1	β_2	β_3	β_4	β_5	β_6	β_7	γ	ϕ	σ
2024-04-16	-1.804×10^{-2}	**3.972×10^{-1}**	**3.721×10^{-1}**	-3.818×10^{-2}	**3.151×10^{-1}**	**-2.022×10^{-1}**	-9.579×10^{-2}	1.208	0.705	1.175
	(9.642×10^{-1})	(8.703×10^{-3})	(8.260×10^{-3})	(2.714×10^{-2})	(3.211×10^{-2})	(3.194×10^{-2})	(9.970×10^{-1})	(9.341×10^{-3})	(3.430×10^{-3})	(6.664×10^{-3})
2024-04-17	3.003×10^{-2}	**3.093×10^{-1}**	**3.077×10^{-1}**	5.204×10^{-3}	**1.695×10^{-1}**	**-8.793×10^{-2}**	-5.692×10^{-1}	1.175	0.776	0.992
	(9.645×10^{-1})	(7.297×10^{-3})	(7.454×10^{-3})	(2.185×10^{-2})	(2.615×10^{-2})	(2.284×10^{-2})	(9.919×10^{-1})	(7.130×10^{-3})	(2.546×10^{-3})	(5.102×10^{-3})
2024-04-18	1.140×10^{-1}	**2.488×10^{-1}**	**2.274×10^{-1}**	**-7.433×10^{-2}**	**1.140×10^{-1}**	-1.574×10^{-2}	-6.585×10^{-1}	1.136	0.795	1.003
	(1.029)	(8.672×10^{-3})	(8.295×10^{-3})	(2.149×10^{-2})	(2.264×10^{-2})	(2.380×10^{-2})	(9.481×10^{-1})	(7.007×10^{-3})	(2.457×10^{-3})	(5.868×10^{-3})
2024-04-19	1.518×10^{-2}	**2.253×10^{-1}**	**2.433×10^{-1}**	3.453×10^{-2}	**9.386×10^{-2}**	**-1.559×10^{-2}**	-5.317×10^{-1}	1.093	0.814	1.024
	(1.032)	(1.042×10^{-2})	(1.143×10^{-2})	(2.369×10^{-2})	(2.825×10^{-2})	(2.636×10^{-2})	(1.024)	(6.072×10^{-3})	(2.498×10^{-3})	(6.003×10^{-3})
2024-04-20	2.429×10^{-2}	**1.383×10^{-1}**	**1.761×10^{-1}**	2.294×10^{-3}	**2.258×10^{-1}**	**-1.773×10^{-1}**	-9.263×10^{-2}	1.054	0.857	1.022
	(9.599×10^{-1})	(1.240×10^{-2})	(1.268×10^{-2})	(5.202×10^{-2})	(5.749×10^{-2})	(5.938×10^{-2})	(1.029)	(5.611×10^{-3})	(1.965×10^{-3})	(5.445×10^{-3})
2024-04-21	1.415×10^{-2}	**2.229×10^{-1}**	**2.352×10^{-1}**	**1.452×10^{-1}**	**2.148×10^{-1}**	**-6.098×10^{-1}**	-5.557×10^{-2}	1.067	0.880	0.982
	(9.928×10^{-1})	(1.270×10^{-2})	(1.350×10^{-2})	(4.685×10^{-2})	(5.521×10^{-2})	(5.991×10^{-2})	(9.951×10^{-1})	(6.195×10^{-3})	(1.856×10^{-3})	(5.385×10^{-3})
2024-04-22	-1.666×10^{-2}	**1.764×10^{-1}**	**1.955×10^{-1}**	**-1.186×10^{-1}**	**3.040×10^{-1}**	**-2.019×10^{-1}**	-6.113×10^{-3}	1.084	0.849	1.025
	(1.012)	(1.070×10^{-2})	(1.020×10^{-2})	(4.456×10^{-2})	(4.809×10^{-2})	(4.974×10^{-2})	(1.008)	(6.366×10^{-3})	(2.184×10^{-3})	(6.296×10^{-3})
2024-04-23	4.351×10^{-2}	**2.802×10^{-1}**	**2.855×10^{-1}**	5.358×10^{-2}	5.447×10^{-2}	**-2.832×10^{-1}**	-1.578×10^{-2}	1.115	0.861	1.040
	(1.015)	(1.134×10^{-2})	(1.133×10^{-2})	(2.829×10^{-2})	(3.263×10^{-2})	(3.519×10^{-2})	(1.029)	(6.161×10^{-3})	(1.775×10^{-3})	(5.275×10^{-3})
2024-04-24	3.409×10^{-3}	**2.456×10^{-1}**	**2.417×10^{-1}**	1.817×10^{-2}	**9.833×10^{-2}**	**-1.957×10^{-1}**	9.305×10^{-2}	1.060	0.875	0.831
	(9.919×10^{-1})	(9.272×10^{-3})	(1.002×10^{-2})	(2.674×10^{-2})	(2.978×10^{-2})	(3.108×10^{-2})	(1.005)	(4.019×10^{-3})	(1.746×10^{-3})	(4.698×10^{-3})
2024-04-25	3.617×10^{-3}	**2.295×10^{-1}**	**2.318×10^{-1}**	4.364×10^{-3}	**2.587×10^{-1}**	**-1.683×10^{-1}**	7.232×10^{-2}	1.076	0.773	1.112
	(1.002)	(8.941×10^{-3})	(9.594×10^{-3})	(3.006×10^{-2})	(3.455×10^{-2})	(3.329×10^{-2})	(1.012)	(8.494×10^{-3})	(3.242×10^{-3})	(8.438×10^{-3})
2024-04-26	-1.341×10^{-2}	**5.818×10^{-2}**	**5.658×10^{-2}**	2.151×10^{-2}	**1.275×10^{-1}**	-5.748×10^{-2}	-6.706×10^{-1}	1.030	0.833	0.972
	(9.938×10^{-1})	(1.001×10^{-2})	(9.939×10^{-3})	(2.780×10^{-2})	(3.318×10^{-2})	(2.987×10^{-2})	(9.684×10^{-1})	(4.720×10^{-3})	(2.089×10^{-3})	(5.099×10^{-3})
2024-04-27	-6.252×10^{-2}	**1.193×10^{-1}**	**1.307×10^{-1}**	-1.006×10^{-1}	**2.045×10^{-1}**	**-1.277×10^{-1}**	-1.815×10^{-1}	0.936	0.903	0.824
	(1.028)	(1.325×10^{-2})	(1.345×10^{-2})	(5.355×10^{-2})	(6.145×10^{-2})	(5.556×10^{-2})	(1.024)	(4.772×10^{-3})	(1.989×10^{-3})	(6.209×10^{-3})
2024-04-28	-3.758×10^{-4}	**1.610×10^{-1}**	**1.798×10^{-1}**	-7.083×10^{-2}	**3.903×10^{-1}**	**-1.758×10^{-1}**	6.224×10^{-2}	0.898	0.893	0.891
	(9.946×10^{-1})	(1.344×10^{-2})	(1.328×10^{-2})	(5.869×10^{-2})	(6.525×10^{-2})	(6.180×10^{-2})	(9.898×10^{-1})	(5.021×10^{-3})	(2.165×10^{-3})	(7.693×10^{-3})
2024-04-29	-1.288×10^{-4}	**1.347×10^{-1}**	**1.020×10^{-1}**	**1.008×10^{-1}**	3.882×10^{-2}	**-2.888×10^{-1}**	-6.546×10^{-2}	1.022	0.827	1.026
	(1.004)	(1.098×10^{-2})	(1.092×10^{-2})	(3.570×10^{-2})	(3.977×10^{-2})	(3.790×10^{-2})	(1.034)	(7.154×10^{-3})	(2.896×10^{-3})	(8.849×10^{-3})
2024-04-30	8.929×10^{-2}	**2.170×10^{-1}**	**1.985×10^{-1}**	3.590×10^{-2}	**1.737×10^{-1}**	**-8.089×10^{-2}**	-8.613×10^{-1}	1.086	0.795	0.988
	(9.952×10^{-1})	(9.880×10^{-3})	(1.029×10^{-2})	(2.016×10^{-2})	(2.393×10^{-2})	(2.192×10^{-2})	(9.876×10^{-1})	(5.057×10^{-3})	(2.555×10^{-3})	(4.569×10^{-3})

The upper number is the posterior mean, and the lower number in parentheses is the posterior standard deviation.

The boldface in the posterior mean indicates that $\boldsymbol{\beta}$ does not include a zero in the 95% credible interval.

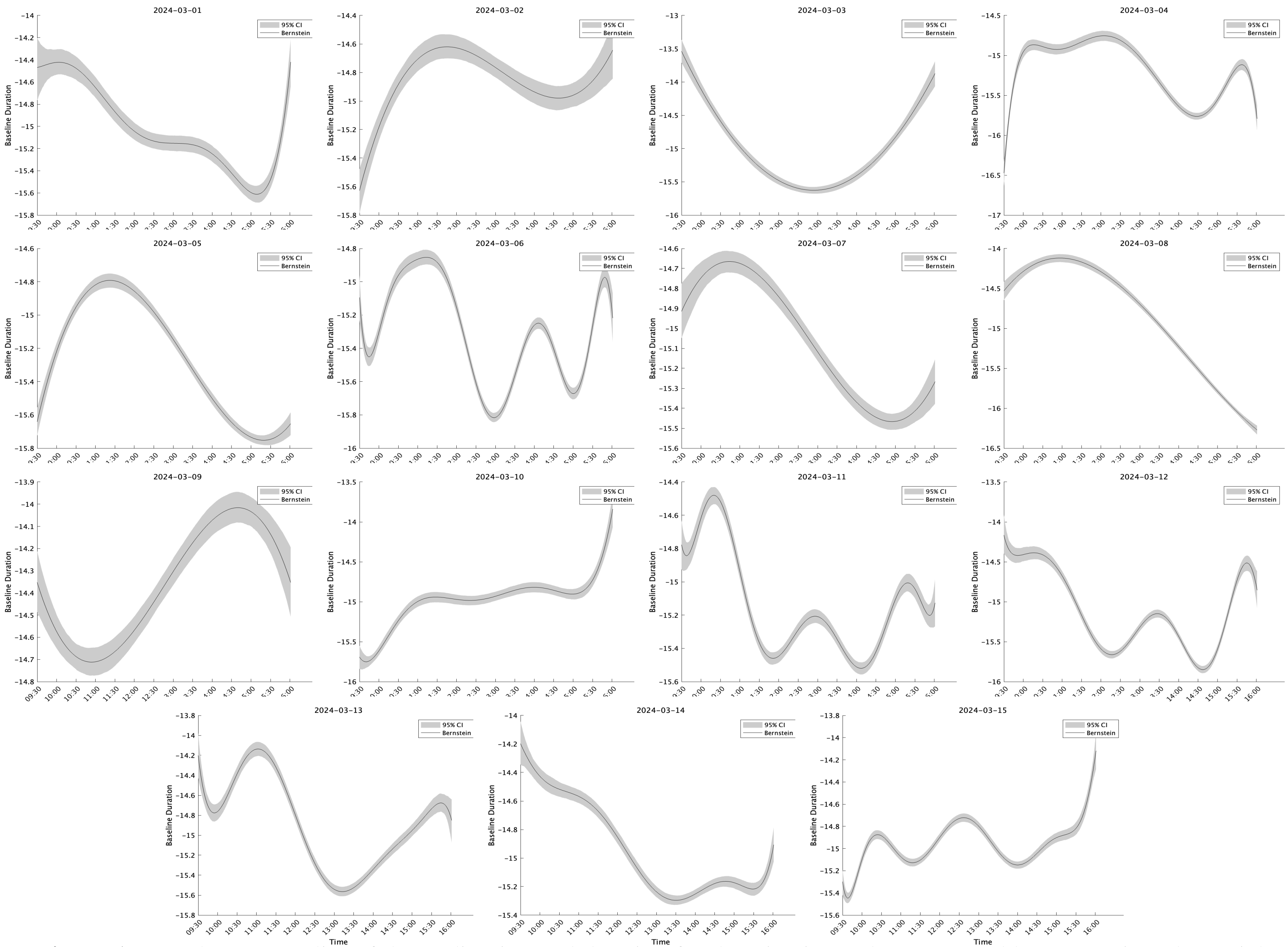

Figure 1. Intraday seasonality of the trading interval duration for the Bitcoin market expressed by Bernstein polynomials (March 2024).

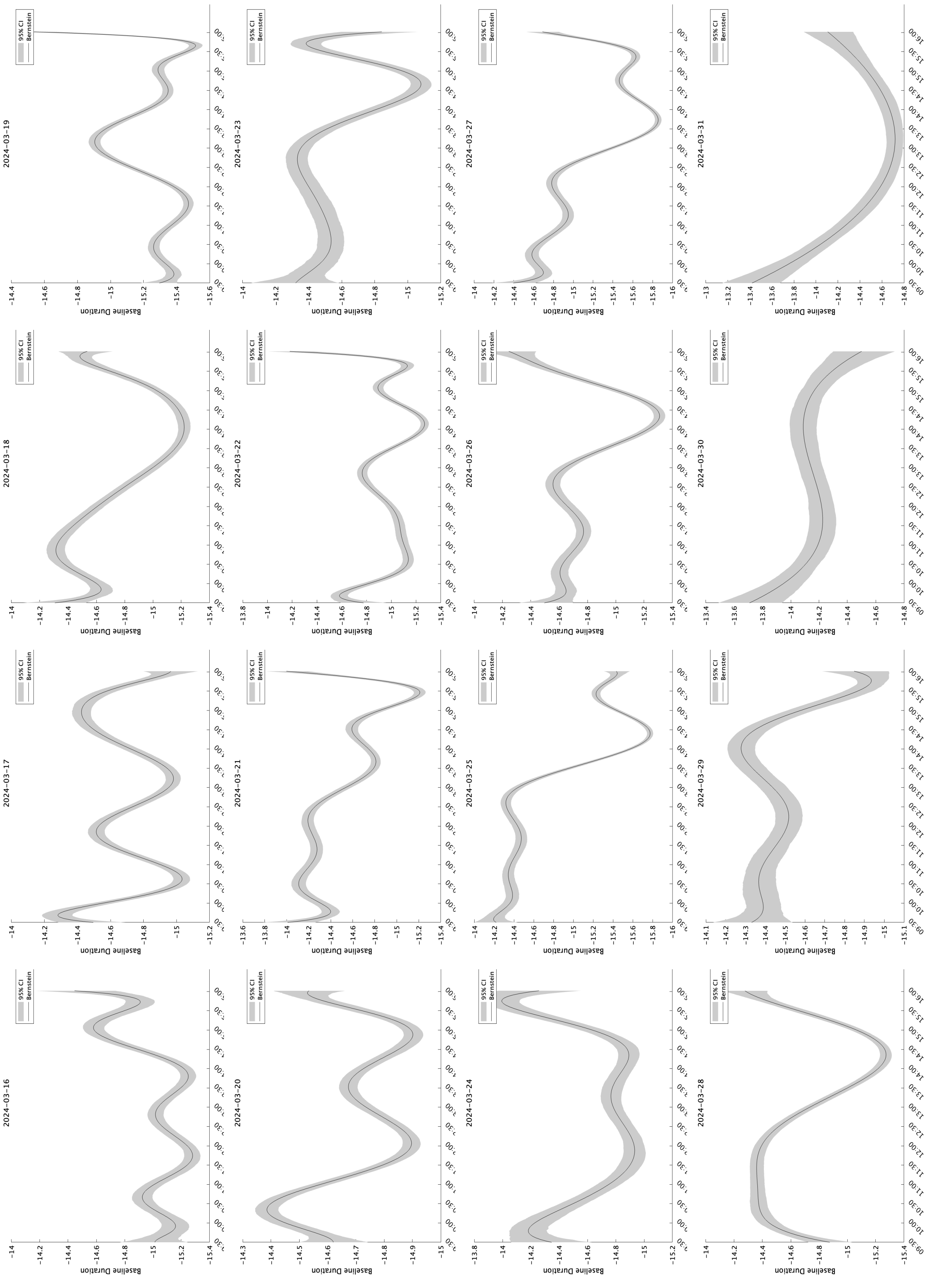

Figure 1. Intraday seasonality of the trading interval duration for the Bitcoin market expressed by Bernstein polynomials (March 2024) (continued).

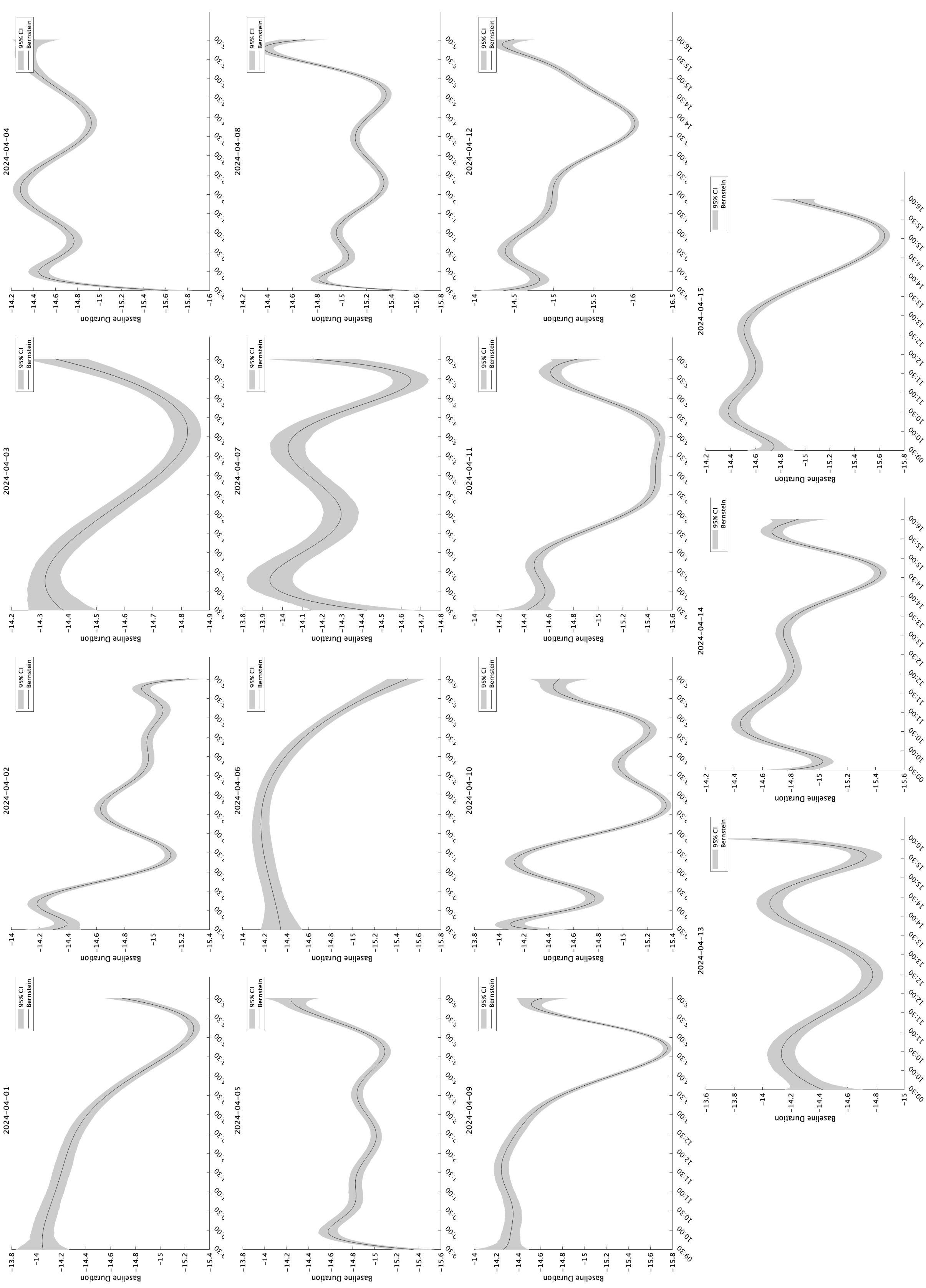

Figure 2. Intraday seasonality of the trading interval duration for the Bitcoin market expressed by Bernstein polynomials (April 2024).

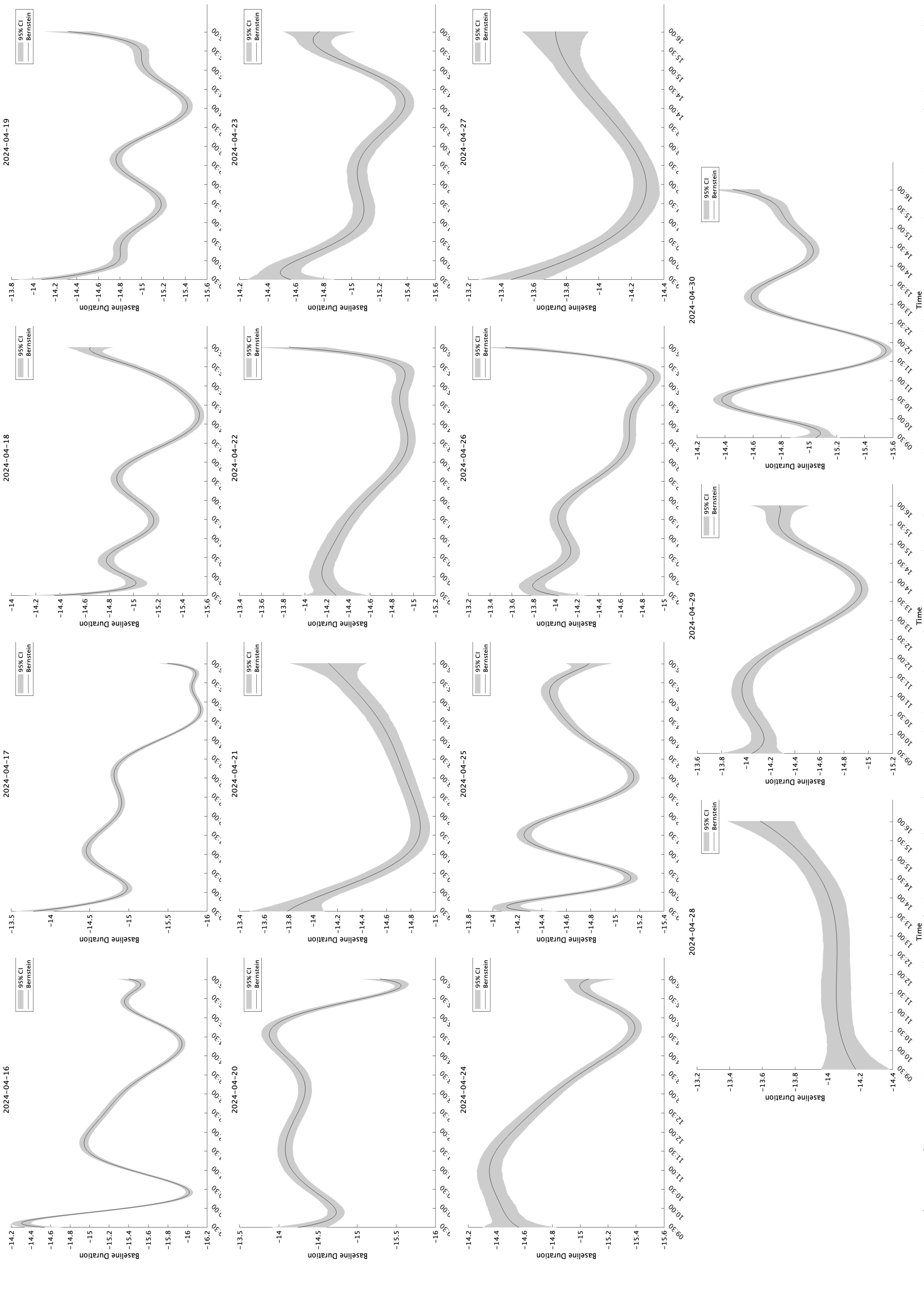

Figure 2. Intraday seasonality of the trading interval duration for the Bitcoin market expressed by Bernstein polynomials (April 2024) (continued).

5. Discussion

In this section, we will discuss the similarities and differences with related literature, as well as future research prospects based on the results.

To the best of the authors' knowledge, there is no literature on the durations of trades in cryptocurrencies using tick data. Since research in this area is still in a developmental stage, there is potential to expand the scope of research, for example, by using other cryptocurrencies such as Ethereum or by using models other than the SCD models for estimation. Also, as mentioned earlier, the trading interval durations and volatility tend to move in conjunction. In our research, we found that the price/return and trading volume of Bitcoin are correlated with the trading interval durations. In our research, we found that the price/return and trading volume of Bitcoin are correlated with the trading interval durations. In contrast, while this research concluded that there is no intraday seasonality in the Bitcoin market, literature concludes that there is volatility in cryptocurrencies (e.g., Ben Omrane et al. (2024); Eross et al. (2019); Shanaev and Ghimire (2022); Su et al. (2022)). Furthermore, Eross et al. (2019) noted that the trading volume and volatility of Bitcoin against the US dollar and euro increased significantly during LNY hours (the hours when both the London and New York markets are open). Su et al. (2022) pointed out that the Bitcoin trading volume decreased from 4 p.m. to midnight. These findings were unrecognized in our research because we focused on the hours when the stock market was open. From these results, although there are issues with computing capacity, if we conduct an analysis without limiting the data, new discoveries may be obtained. In addition, while literature has shown that there are day-of-the-week effects on volatility (Aharon and Qadan (2019)) and within-the-month effects on pricing efficiency (Qadan et al. (2022)), there are no such effects on trading interval durations based on our results.

From those results, although the duration and volatility are seemingly linked, it is more natural to think of them as being driven by one or more third variable(s) rather than causality. In this research, we used variables related to return, price change, and volume, but other data can also be considered as candidates for explanatory variables. Also, there may be special phenomena in the cryptocurrency market, such as volatility cascades (e.g., Gradojevic and Tsiakas (2021); Brini and Lenz (2024)), where the trading interval durations have a chain-like effect. Furthermore, we can also explore ways of extracting data.

There are also other ways of collecting data that could be considered. This research analyzed the durations of all trades within the target period, but it is also possible to limit the trades themselves that are recorded. For instance, by limiting the data to only trades that occurred when a price change occurred, or only trades above a certain volume, it may be possible to obtain additional findings. In the field of volatility, there is a method that uses data that only records trades that represent significant price changes in the opposite direction of the trend, and its usefulness has been demonstrated (e.g., Tsang et al. (2016); Tsang (2021)).

6. Conclusions

In this study, we used the SCD model to analyze trading interval durations in the Bitcoin market incorporating the trade price and trade volume as explanatory variables and including a Bernstein polynomial to consider the possibility of intraday seasonality and control for coincidental temporal trends. Our objective was to clarify the characteristics of Bitcoin and identify similarities and differences compared with other conventional financial assets such as stocks and commodities. Because the posterior distributions of the model parameters could be derived analytically, we used the MCMC method to estimate them numerically.

In the Bitcoin market, the relationship between price changes/return and trading interval duration was not observed. However, we found that positive relationships existed between the dummy variables for price increases/decreases and trade interval durations. In other words, the trading interval duration was longer in cases when the price increased or decreased compared to cases when the price did not change. In addition, on the one hand, the cross-term of the dummy variable for price increases and the trading volume also had a positive relationship with the trading interval, indicating that the trading interval was longer when the trading volume was larger in cases when the price increased. On the other hand, the cross-term of the dummy variable for price decreases and the trading volume was negatively related to the trading interval durations, showing that when prices fall, the larger the trading volume, the shorter the trading interval duration becomes.

This result is similar to the leverage effect commonly exhibited in financial markets. Note that while volatility is negatively correlated with the price decline, it was revealed that the duration of Bitcoin trades is affected by the trading volume when the price is negative rather than by the price decline itself. In addition, the effect of the trade volume itself was not statistically significant in many cases, and the effect was limited depending on the market conditions.

With regard to the period when the stock market is open, no common intraday seasonality was observed in the Bitcoin trading durations. Since the Bitcoin market is open 24 hours a day, 365 days a year, traders do not need to rush to place orders immediately after the opening or just before the closing of the stock or commodity markets. At the same time, however, the strong persistence typically seen in conventional financial assets was also observed in the Bitcoin market, so we conclude that the Bitcoin trading interval durations have both characteristics similar to and dissimilar from those of conventional financial assets.

A. Appendix

A.1. Conditional posterior distributions

A.1.1. State variable $\boldsymbol{\alpha}$

The conditional posterior distribution of the state variable $\boldsymbol{\alpha}$ is given by

$$p(\boldsymbol{\alpha}|\theta, \boldsymbol{y}, X) \propto \prod_{i=1}^{n} p(y_i|\alpha_i, \boldsymbol{\beta}, \gamma, \boldsymbol{x}_i) \cdot p(\boldsymbol{\alpha}|\phi, \sigma^2). \tag{12}$$

To generate $\boldsymbol{\alpha}$ from Equation (12), we apply the Metropolis–Hastings (MH) algorithm. To derive an appropriate proposal distribution for the MH algorithm, we can consider

$$\ell(\boldsymbol{\alpha}) \equiv \sum_{i=1}^{n} \log p(y_i|\alpha_i, \boldsymbol{\beta}, \gamma), \tag{13}$$

$$\log p(y_i|\alpha_i, \boldsymbol{\beta}, \gamma) = \log\gamma - \log y_i + \gamma(\log y_i - \boldsymbol{x}_i'\boldsymbol{\beta} - \alpha_i) - \exp\left(\gamma(\log y_i - \boldsymbol{x}_i'\boldsymbol{\beta} - \alpha_i)\right) \tag{14}$$

in the neighborhood of $\boldsymbol{\alpha}^* = \left[\alpha_1^* \ \ldots \ \alpha_n^*\right]'$. Then,

$$\ell(\boldsymbol{\alpha}) \approx \ell(\boldsymbol{\alpha}^*) + \boldsymbol{g}(\boldsymbol{\alpha} - \boldsymbol{\alpha}^*) - \frac{1}{2}(\boldsymbol{\alpha} - \boldsymbol{\alpha}^*)'Q(\boldsymbol{\alpha} - \boldsymbol{\alpha}^*), \tag{15}$$

where $\boldsymbol{g}(\boldsymbol{\alpha})$ is the gradient vector of $\ell(\boldsymbol{\alpha})$ and $Q(\boldsymbol{\alpha})$ is the Hessian matrix of $\ell(\boldsymbol{\alpha})$ times -1. Then, we have

$$\begin{aligned}\boldsymbol{g}(\boldsymbol{\alpha}^*) &\equiv \nabla_\alpha \ell(\boldsymbol{\alpha}^*) = [g_1(\boldsymbol{\alpha}^*), \ldots, g_n(\boldsymbol{\alpha}^*)]', \\ Q(\boldsymbol{\alpha}^*) &\equiv -\nabla_\alpha \nabla_\alpha' \ell(\boldsymbol{\alpha}^*) = \mathrm{diag}\{q_1(\boldsymbol{\alpha}^*), \ldots, q_n(\boldsymbol{\alpha}^*)\},\end{aligned}$$

where

$$\begin{aligned}g_i(\boldsymbol{\alpha}^*) &= -\gamma + \gamma \exp\left(\gamma(\log y_i = \boldsymbol{x}_i'\boldsymbol{\beta} - \alpha_i^*)\right), \\ q_i(\boldsymbol{\alpha}^*) &= \gamma^2 \exp\left(\gamma(\log y_i - \boldsymbol{x}_i'\boldsymbol{\beta} - \alpha_i^*)\right).\end{aligned}$$

With the prior distribution of $\boldsymbol{\alpha} \sim \text{Normal}\left(\boldsymbol{\mu}_\alpha, \Sigma_\alpha^{-1}\right)$, the conditional posterior distribution of $\boldsymbol{\alpha}$ can be approximated as

$$\begin{aligned}p(\boldsymbol{\alpha}|\theta, \boldsymbol{y}, X) &= C\exp\left[\ell(\boldsymbol{\alpha}) + \log p(\boldsymbol{\alpha})\right] \\ &\approx C\exp\left[\ell(\boldsymbol{\alpha}^*) + \boldsymbol{g}(\boldsymbol{\alpha}^*)'(\boldsymbol{\alpha} - \boldsymbol{\alpha}^*) - \frac{1}{2}(\boldsymbol{\alpha} - \boldsymbol{\alpha}^*)'Q(\boldsymbol{\alpha}^*)(\boldsymbol{\alpha} - \boldsymbol{\alpha}^*) + \log p(\boldsymbol{\alpha})\right] \\ &= C\exp\left[\ell(\boldsymbol{\alpha}^*) - \frac{n}{2}\log(2\pi\sigma^2) + \frac{1}{2}\log(1 - \phi^2)\right] \\ &\quad \times \exp\left[\boldsymbol{g}(\boldsymbol{\alpha}^*)'(\boldsymbol{\alpha} - \boldsymbol{\alpha}^*) - \frac{1}{2}(\boldsymbol{\alpha} - \boldsymbol{\alpha}^*)'Q(\boldsymbol{\alpha}^*)(\boldsymbol{\alpha} - \boldsymbol{\alpha}^*) - \frac{1}{2\sigma^2}\boldsymbol{\alpha}'V\boldsymbol{\alpha}\right],\end{aligned} \tag{16}$$

where C is a normalizing constant. By completing the square for the exponential of Equation (16) with respect to $\boldsymbol{\alpha}$, we obtain

$$\begin{aligned}&\boldsymbol{g}(\boldsymbol{\alpha}^*)'(\boldsymbol{\alpha} - \boldsymbol{\alpha}^*) - \frac{1}{2}(\boldsymbol{\alpha} - \boldsymbol{\alpha}^*)'Q(\boldsymbol{\alpha}^*)(\boldsymbol{\alpha} - \boldsymbol{\alpha}^*) - \frac{1}{2\sigma^2}\boldsymbol{\alpha}'V\boldsymbol{\alpha} \\ &= -\frac{1}{2}\left(\boldsymbol{\alpha} - \boldsymbol{\mu}_\alpha(\boldsymbol{\alpha}^*)\right)'\Sigma_\alpha(\boldsymbol{\alpha}^*)^{-1}\left(\boldsymbol{\alpha} - \boldsymbol{\mu}_\alpha(\boldsymbol{\alpha}^*)\right) + \frac{1}{2}\boldsymbol{g}(\boldsymbol{\alpha}^*)'Q(\boldsymbol{\alpha}^*)^{-1}\boldsymbol{g}(\boldsymbol{\alpha}^*) \\ &\quad - \frac{1}{2}\left(\boldsymbol{g}(\boldsymbol{\alpha}^*) + Q(\boldsymbol{\alpha}^*)\boldsymbol{\alpha}^*\right)'\left(\Sigma_\alpha + Q(\boldsymbol{\alpha}^*)^{-1}\right)\left(\boldsymbol{g}(\boldsymbol{\alpha}^*) + Q(\boldsymbol{\alpha}^*)\boldsymbol{\alpha}^*\right),\end{aligned} \tag{17}$$

where

$$\Sigma_\alpha(\boldsymbol{\alpha}^*) = \left(\frac{1}{\sigma^2}V + Q(\boldsymbol{\alpha}^*)\right)^{-1}, \quad \boldsymbol{\mu}_\alpha(\boldsymbol{\alpha}^*) = \Sigma_\alpha(\boldsymbol{\alpha}^*)\left(\boldsymbol{g}(\boldsymbol{\alpha}^*) + Q(\boldsymbol{\alpha}^*)\boldsymbol{\alpha}^*\right).$$

Therefore, the right-hand side of Equation (16) is approximately proportional to

$$\boldsymbol{\alpha} \sim \text{Normal}(\boldsymbol{\mu}_\alpha(\boldsymbol{\alpha}^*), \Sigma_\alpha(\boldsymbol{\alpha}^*)) \tag{18}$$

Then, by using Equation (18) as the proposal distribution, we can apply the MH algorithm to generate $\boldsymbol{\alpha}$. However, there are two practical issues that need to be addressed:

- An appropriate $\boldsymbol{\alpha}^*$ needs to be selected to make the approximation of Equation (16) practical.
- The MH algorithm tends to have a low acceptance rate because $\boldsymbol{\alpha}$ is a high-dimensional vector.

To deal with the former problem, we set the mode of the conditional posterior probability as $\boldsymbol{\alpha}^*$. To search for the mode, the following recursive algorithm was employed:

Step 1: Initialize $\boldsymbol{\alpha}^{*(0)}$, and set the counter $r = 1$.

Step 2: Update $\boldsymbol{\alpha}^{*(r)}$ by $\boldsymbol{\alpha}^{*(r)} = \boldsymbol{\mu}_\alpha\left(\boldsymbol{\alpha}^{*(r-1)}\right)$.

Step 3: Let $r = r + 1$, and go to **Step 2** unless $\max_{i,\ldots,n}\left|\alpha_i^{*(r)} - \alpha_i^{*(r-1)}\right|$ is less than the preset tolerance level.

This algorithm is equivalent to the Newton–Raphson method and thus converges in a few iterations. To solve the latter problem, we applied the block sampler proposed by Shepard and Pitt (1997) and Watanabe and Omori (2004), where the $\boldsymbol{\alpha}$ is randomly divided into two subvectors (blocks). Then, the MH algorithm is applied to each subvector with one subvector as $\boldsymbol{\alpha}_b$ and the other subvector as $\boldsymbol{\alpha}_r$:

$$\boldsymbol{\alpha} = \begin{pmatrix}\boldsymbol{\alpha}_b\\ \boldsymbol{\alpha}_r\end{pmatrix}, \quad \boldsymbol{\alpha}^* = \begin{pmatrix}\boldsymbol{\alpha}_b^*\\ \boldsymbol{\alpha}_r^*\end{pmatrix}, \quad \Sigma_\alpha(\boldsymbol{\alpha}^*)^{-1} = \begin{pmatrix}\Omega_{bb} & \Omega_{br}\\ \Omega_{rb} & \Omega_{rr}\end{pmatrix}. \tag{19}$$

By using Equations (18) and (19), the kernel of the conditional distribution $p(\boldsymbol{\alpha}_b|\boldsymbol{\alpha}_r)$ is given by

$$\begin{aligned}
&(\boldsymbol{\alpha} - \boldsymbol{\alpha}^*)'\Sigma_\alpha(\boldsymbol{\alpha}^*)^{-1}(\boldsymbol{\alpha} - \boldsymbol{\alpha}^*)\\
&= \begin{pmatrix}\boldsymbol{\alpha}_b - \boldsymbol{\alpha}_b^*\\ \boldsymbol{\alpha}_r - \boldsymbol{\alpha}_r^*\end{pmatrix}' \begin{pmatrix}\Omega_{bb} & \Omega_{br}\\ \Omega_{rb} & \Omega_{rr}\end{pmatrix} \begin{pmatrix}\boldsymbol{\alpha}_b - \boldsymbol{\alpha}_b^*\\ \boldsymbol{\alpha}_r - \boldsymbol{\alpha}_r^*\end{pmatrix} \qquad .\\
&= (\boldsymbol{\alpha}_b - \boldsymbol{\alpha}_b^*)'\Omega_{bb}\boldsymbol{\alpha}_b - \boldsymbol{\alpha}_b^* + 2(\boldsymbol{\alpha}_r - \boldsymbol{\alpha}_r^*)'\Omega_{rb}(\boldsymbol{\alpha}_b - \boldsymbol{\alpha}_b^*) + (\boldsymbol{\alpha}_r - \boldsymbol{\alpha}_r^*)'\Omega_{rr}(\boldsymbol{\alpha}_r - \boldsymbol{\alpha}_r^*)
\end{aligned} \tag{20}$$

By completing the square of Equation (20), we get

$$\begin{aligned}
&(\boldsymbol{\alpha}_b - \boldsymbol{\alpha}_b^*)'\Omega_{bb}(\boldsymbol{\alpha}_b - \boldsymbol{\alpha}_b^*) + 2(\boldsymbol{\alpha}_r - \boldsymbol{\alpha}_r^*)'\Omega_{rb}(\boldsymbol{\alpha}_b - \boldsymbol{\alpha}_b^*) + (\boldsymbol{\alpha}_{-}\boldsymbol{\alpha}_r^*)'\Omega_{rr}(\boldsymbol{\alpha}_r - \boldsymbol{\alpha}_r^*)\\
&= \left(\boldsymbol{\alpha}_b - \boldsymbol{\mu}_{\alpha_b}(\boldsymbol{\alpha}^*)\right)'\Sigma_{\alpha_b}\left(\boldsymbol{\alpha}_b - \boldsymbol{\mu}_{\alpha_b}(\boldsymbol{\alpha}^*)\right) - 2(\boldsymbol{\alpha}_r - \boldsymbol{\alpha}_r^*)'\Omega_{rb}\boldsymbol{\alpha}_b^* + (\boldsymbol{\alpha}_r - \boldsymbol{\alpha}_r^*)'\left(\Omega_{rr} - \Omega_{rb}\Omega_{bb}^{-1}\Omega_{br}\right)(\boldsymbol{\alpha}_r - \boldsymbol{\alpha}_r^*),
\end{aligned} \tag{21}$$

where

$$\boldsymbol{\mu}_{\alpha_b}(\boldsymbol{\alpha}^*) = \boldsymbol{\alpha}_b^* - \Omega_{bb}^{-1}\Omega_{br}(\boldsymbol{\alpha}_r - \boldsymbol{\alpha}_r^*), \quad \Sigma_{\alpha_b}(\boldsymbol{\alpha}^*) = \Omega_{bb}^{-1}.$$

Therefore, the conditional distribution of $\boldsymbol{\alpha}_b$ given by $\boldsymbol{\alpha}_r$ in Equation (20) is rearranged as

$$\boldsymbol{\alpha}_b|\boldsymbol{\alpha}_r \sim \text{Normal}\left(\boldsymbol{\mu}_{\alpha_b}(\boldsymbol{\alpha}^*), \Sigma_{\alpha_b}(\boldsymbol{\alpha}^*)\right) \tag{22}$$

We applied the MH algorithm by dividing $\boldsymbol{\alpha}$ into a random number of blocks from 20 to 40 for each iteration of the sampling scheme.

A.1.2. Regression coefficient $\boldsymbol{\beta}$

The sampling strategy for the regression coefficient $\boldsymbol{\beta}$ is almost identical to the one for the state variable $\boldsymbol{\alpha}$. Let $\ell(\boldsymbol{\beta})$ denote $\log p(\boldsymbol{y}|\theta, X)$. In the same manner as Equation (13), the second-order Taylor approximation of $\ell(\boldsymbol{\beta})$ in the neighborhood of $\boldsymbol{\beta}^*$ is given by

$$\ell(\boldsymbol{\beta}) \approx \ell(\boldsymbol{\beta}^*) + \boldsymbol{\beta}(\boldsymbol{\beta}^*)'(\boldsymbol{\beta} - \boldsymbol{\beta}^*) - \frac{1}{2}(\boldsymbol{\beta} - \boldsymbol{\beta}^*)' Q(\boldsymbol{\beta}^*)(\boldsymbol{\beta} - \boldsymbol{\beta}^*), \tag{23}$$

where $\boldsymbol{g}(\boldsymbol{\beta})$ is the gradient vector of $\ell(\boldsymbol{\beta})$ and $Q(\boldsymbol{\beta})$ is the Hessian matrix of $\ell(\boldsymbol{\beta})$ times -1. Then, we obtain

$$\begin{aligned} \boldsymbol{g}(\boldsymbol{\beta}^*) &\equiv \nabla_\alpha \ell(\boldsymbol{\beta}^*) = \sum_{i=1}^n g_i(\boldsymbol{\beta}^*)\boldsymbol{x}_i \\ Q(\boldsymbol{\beta}^*) &\equiv -\nabla_\alpha \nabla_\beta' \ell(\boldsymbol{\beta}^*) = \sum_{i=1}^n q_i(\boldsymbol{\beta}^*)\boldsymbol{x}_i\boldsymbol{x}_i', \end{aligned}$$

where

$$\begin{aligned} g_i(\boldsymbol{\beta}^*) &= -\gamma + \gamma \exp\left(\gamma(\log y_i - \boldsymbol{x}_i'\boldsymbol{\beta}^* = \alpha_i)\right), \\ q_i(\boldsymbol{\beta}^*) &= \gamma^2 \exp\left(\gamma(\log y_i - \boldsymbol{x}_i'\boldsymbol{\beta}^* - \alpha_i)\right). \end{aligned}$$

With the prior distribution of $\boldsymbol{\beta} \sim \text{Normal}\left(\boldsymbol{\mu}_\beta, \Sigma_\beta^{-1}\right)$, the conditional posterior distribution of $\boldsymbol{\beta}$ can be approximated by

$$\begin{aligned} p(\boldsymbol{\beta}|\theta_{-\beta}, \boldsymbol{y}, X) &= C \exp\left[\ell(\boldsymbol{\beta}) + \log p(\boldsymbol{\beta})\right] \\ &\approx C \exp\left[\ell(\boldsymbol{\beta}^*) + \boldsymbol{g}(\boldsymbol{\beta}^*)'(\boldsymbol{\beta} - \boldsymbol{\beta}^*) - \frac{1}{2}(\boldsymbol{\beta} - \boldsymbol{\beta}^*)' Q(\boldsymbol{\beta}^*)(\boldsymbol{\beta} - \boldsymbol{\beta}^*) + \log p(\boldsymbol{\beta})\right] \\ &= C \exp\left[\ell(\boldsymbol{\beta}^*) - \frac{1}{2}\log(2\pi) + \frac{1}{2}\log|\Sigma_\beta|\right] \\ &\quad \times \exp\left[\boldsymbol{g}(\boldsymbol{\beta}^*)'(\boldsymbol{\beta} - \boldsymbol{\beta}^*) - \frac{1}{2}(\boldsymbol{\beta} - \boldsymbol{\beta}^*)' Q(\boldsymbol{\beta}^*)(\boldsymbol{\beta} - \boldsymbol{\beta}^*) - \frac{1}{2}\left(\boldsymbol{\beta} - \boldsymbol{\mu}_\beta\right)' \Sigma_\beta \left(\boldsymbol{\beta} - \boldsymbol{\mu}_\beta\right)\right], \end{aligned} \tag{24}$$

where C is a normalizing constant. By completing the square for the exponential of Equation (24) with respect to $\boldsymbol{\beta}$, we obtain

$$\begin{aligned}
&\boldsymbol{g}(\boldsymbol{\beta}^*)'(\boldsymbol{\beta}-\boldsymbol{\beta}^*) - \frac{1}{2}(\boldsymbol{\beta}-\boldsymbol{\beta}^*)'Q(\boldsymbol{\beta}^*)(\boldsymbol{\beta}-\boldsymbol{\beta}^*) - \frac{1}{2}\left(\boldsymbol{\beta}-\boldsymbol{\mu}_\beta\right)'\Sigma_\beta\left(\boldsymbol{\beta}-\boldsymbol{\mu}_\beta\right) \\
&= -\frac{1}{2}\left(\boldsymbol{\beta}-\boldsymbol{\mu}_\beta(\boldsymbol{\beta}^*)\right)'\Sigma_\beta(\boldsymbol{\beta}^*)^{-1}\left(\boldsymbol{\beta}-\boldsymbol{\mu}_\beta(\boldsymbol{\beta}^*)\right) + \frac{1}{2}\boldsymbol{g}(\boldsymbol{\beta}^*)'Q(\boldsymbol{\beta}^*)^{-1}\boldsymbol{g}(\boldsymbol{\beta}^*) \\
&\quad - \frac{1}{2}\left(\boldsymbol{g}(\boldsymbol{\beta}^*) + Q(\boldsymbol{\beta}^*)\boldsymbol{\beta}^*\right)'\left(\Sigma_\beta + Q(\boldsymbol{\beta}^*)^{-1}\right)\left(\boldsymbol{g}(\boldsymbol{\beta}^*) + Q(\boldsymbol{\beta}^*)\boldsymbol{\beta}^*\right),
\end{aligned} \tag{25}$$

where

$$\Sigma_\beta(\boldsymbol{\beta}^*) = \left(\Sigma_\beta + Q(\boldsymbol{\beta}^*)\right)^{-1}, \quad \boldsymbol{\mu}_\beta(\boldsymbol{\beta}^*) = \Sigma_\beta(\boldsymbol{\beta}^*)\left(\Sigma_\beta\boldsymbol{\mu}_\beta + \boldsymbol{g}(\boldsymbol{\beta}^*) + Q(\boldsymbol{\beta}^*)\boldsymbol{\beta}^*\right).$$

Therefore, the right-hand side of Equation (24) is approximately proportional to

$$\boldsymbol{\beta} \sim \text{Normal}(\boldsymbol{\mu}_\beta(\boldsymbol{\beta}^*), \Sigma_\beta(\boldsymbol{\beta}^*)) \tag{26}$$

The search algorithm for $\boldsymbol{\beta}^*$ is the same as for $\boldsymbol{\alpha}$. Contrary to $\boldsymbol{\alpha}$, however, $\boldsymbol{\beta}$ has a small number of dimensions, so the block sampler is not applied.

A.1.3. Shape parameter γ

The sampling strategy for the shape parameter γ is almost the same as for $\boldsymbol{\alpha}$ and $\boldsymbol{\beta}$. Because the prior distribution of γ is not a normal distribution, we consider the log conditional posterior distribution of γ instead of Equation (13). Let

$$f(\gamma) \equiv \sum_{i=1}^{n} \log p(y_i|\alpha_i, \boldsymbol{\beta}, \gamma) + \log p(\gamma) + \text{constant}. \tag{27}$$

Then, the second-order Taylor expansion of Equation (27) with respect to γ in the neighborhood of $\gamma^* > 0$ is given by

$$f(\gamma) \approx f(\gamma^*) + g(\gamma^*)(\gamma-\gamma^*) - \frac{1}{2}q(\gamma^*)(\gamma-\gamma^*)^2, \tag{28}$$

where

$$\begin{aligned}
g(\gamma^*) &\equiv \nabla_\gamma f(\gamma^*) \\
&= \frac{n}{\gamma^*} + \sum_{i=1}^{n}\left(u_i - u_i e^{\gamma^* u_i}\right) + \frac{a_\gamma - 1}{\gamma^*} - b_\gamma, \\
q(\gamma^*) &\equiv -\nabla_\gamma^2 f(\gamma^*)
\end{aligned}$$

$$= \frac{n}{\gamma^{*2}} + \sum_{i=1}^{n} u_i^2 e^{\gamma^* u_i} + \frac{a_\gamma - 1}{\gamma^{*2}},$$
$$u_i \equiv \log y_i - \boldsymbol{x}_i'\boldsymbol{\beta} - \alpha_i, \quad i \in \{1, \ldots, n\}.$$

Here, $q(\gamma^*)$ is positive for any $\gamma^* > 0$ if $n + a_\gamma > 1$.

By completing the square of Equation (27), we get the proposed distribution

$$\gamma \sim \text{Normal}\left(\mu_\alpha(\gamma^*), \sigma_\gamma^2(\gamma^*)\right), \tag{29}$$

where

$$\sigma_\gamma^2(\gamma^*) = \frac{1}{q(\gamma^*)}, \quad \mu_\gamma(\gamma^*) = \gamma^* + \frac{g(\gamma^*)}{q(\gamma^*)}$$

Because of the global concavity of $f(\gamma)$, if we use the mode of $f(\gamma)$ as γ^*, $g(\gamma^*) = 0$ always holds. Therefore, $\mu_\gamma(\gamma^*)$ is practically the same as γ^*.

A.1.4. AR(1) coefficient ϕ

Once the state variable $\boldsymbol{\alpha}$ is generated, the conditional posterior distribution of ϕ is given by

$$\begin{aligned} p(\phi|\boldsymbol{y}, \boldsymbol{\alpha}, \phi) &\propto p(\boldsymbol{\alpha}|\phi, \sigma^2)p(\phi) \\ &\propto \sqrt{1-\phi^2}\exp\left[-\frac{(1-\phi^2)\alpha_1^2 + \sum_{i=2}^{n}(\alpha_i - \phi\alpha_{i-1})^2}{2\sigma^2}\right] \times (1+\phi)^{a_\phi - 1}(1-\phi)^{b_\phi - 1}. \end{aligned} \tag{30}$$

By completing the square for the exponential, we obtain

$$\begin{aligned} (1-\phi^2)\alpha_1^2 + \sum_{i=2}^{n}(\alpha_i - \phi\alpha_{i=1})^2 &= (1-\phi^2)\alpha_1^2 + \sum_{i=2}^{n}\alpha_i^2 - 2\phi\sum_{i=2}^{n}\alpha_i\alpha_{i-1} + \phi^2\sum_{i=2}^{n}\alpha_{i-1}^2 \\ &= \alpha_1^2 + \sum_{i=2}^{n}\alpha_i^2 - 2\phi\sum_{i=2}^{n}\alpha_i\alpha_{i-1} + \phi^2\sum_{i=2}^{n-1}\alpha_i^2 \\ &= \sum_{i=2}^{n-1}\alpha_i^2\left(\phi - \frac{\sum_{i=2}^{n}\alpha_i\alpha_{i-1}}{\sum_{i=2}^{n-1}\alpha_i^2}\right)^2 + \alpha_1^2 - \frac{(\sum_{i=2}^{n}\alpha_i\alpha_{i-1})^2}{\sum_{i=2}^{n-1}\alpha_i^2}. \end{aligned}$$

With the above expression in mind, we can use the following normal distribution as the proposal distribution for ϕ in the MH algorithm:

$$\phi \sim \text{Normal}\left(\frac{\sum_{i=2}^{n}\alpha_i\alpha_{i-1}}{\sum_{i=2}^{n-1}\alpha_i^2}, \frac{\sigma^2}{\sum_{i=2}^{n-1}\alpha_i^2}\right). \tag{31}$$

A.1.5. Variance σ^2

Because we used the standard conditionally conjugate prior distribution for σ^2, the conditional posterior distribution of σ^2 is given by

$$\begin{aligned} p(\sigma^2|\boldsymbol{y}, \boldsymbol{\alpha}, \phi) &\propto p(\boldsymbol{\alpha}|\phi, \sigma^2)p(\sigma^2) \\ &\propto \exp\left[-\frac{n}{2}\log\sigma^2 - \frac{1}{2\sigma^2}\boldsymbol{\alpha}'V\boldsymbol{\alpha}\right] \times (\sigma^2)^{-a_\sigma-1}\exp\left(-\frac{b_\sigma}{\sigma^2}\right) \\ &= (\sigma^2)^{-\sigma_a-\frac{n}{2}-1}\exp\left(-\frac{b_\sigma + \frac{1}{2}\boldsymbol{\alpha}'V\boldsymbol{\alpha}}{\sigma^2}\right). \end{aligned} \tag{32}$$

Because Equation (32) is the kernel of the posterior distribution of σ^2, it is derived as

$$\sigma^2|\boldsymbol{y}, \boldsymbol{\alpha}, \phi \sim \text{Inv. Gamma}\left(a_\sigma + \frac{n}{2}, b_\sigma + \frac{1}{2}\boldsymbol{\alpha}'V\boldsymbol{\alpha}\right). \tag{33}$$

A.2. Centered parametrization (CP) form

Appendix A.1 presents the conditional posterior distributions for the model parameters. Although these distributions can be estimated by the MCMC method, the generated samples would have strong autocorrelation, which would result in low sampling efficiency. To improve the sampling efficiency, we employed the ancillarity-sufficiency interweaving strategy (ASIS) proposed by Yu and Meng (2011), which is an algorithm that samples from two different but essentially equal models of parameterizations. In this study, we set one model as the original model in Appendix A.1 and the other model is to be centered on the missing/latent variables of the original model (i.e., $\boldsymbol{\alpha}$). We defined the original SCD model in Equations (1) and (2) as the non-centered parameterization (NCP) form and the centered model as the centered parameterization (CP) form.

We can implement the following conversion with respect to α_i:

$$\tilde{\alpha}_i = \alpha_i - \boldsymbol{x}_i'\boldsymbol{\beta}. \tag{34}$$

Then, the SCD model in Equations (1) and (2) becomes

$$y_i = \exp(\tilde{\alpha}_i)\,\varepsilon_i, \quad \varepsilon_i > 0, \quad i \in \{1, \ldots, N\}, \tag{35}$$

$$\begin{aligned} \tilde{\alpha}_i - \boldsymbol{x}_i'\boldsymbol{\beta} &= \phi(\tilde{\alpha}_{i-1} - \boldsymbol{x}_{i-1}'\boldsymbol{\beta}) + \eta_i \\ \eta_i &\sim \text{Normal}(0, \sigma^2), \quad i \in \{2, \ldots, N\}. \end{aligned} \tag{36}$$

The likelihood for the SCD model in Equations (35) and (36) given the observation $\boldsymbol{y}$ and latent variable $\tilde{\boldsymbol{\alpha}}$ is expressed as

$$p(\boldsymbol{y}, \tilde{\boldsymbol{\alpha}}|\theta) = \underbrace{\prod_{i=1}^{n} p(y_i|\tilde{\alpha}_i, \gamma)}_{p(\boldsymbol{y}|\tilde{\boldsymbol{\alpha}},\theta)} \cdot \underbrace{p(\tilde{\alpha}_1|\boldsymbol{\beta}, \phi, \sigma^2, X)\prod_{i=2}^{n} p(\tilde{\alpha}_i|\tilde{\alpha}_{i-1}, \boldsymbol{\beta}, \phi, \sigma^2, X)}_{p(\tilde{\boldsymbol{\alpha}}|\theta,X)}, \tag{37}$$

where

$$p(y_i|\tilde{\alpha}_i,\gamma) = \gamma y_i^{\gamma-1}\exp\left(-\gamma\tilde{\alpha}_i - y_i^{\gamma}\exp(-\gamma\tilde{\alpha}_i)\right), \tag{38}$$

$$p(\tilde{\alpha}_1|\boldsymbol{\beta},\phi,\sigma^2,X) = \sqrt{\frac{1-\phi^2}{2\pi\sigma^2}}\exp\left[-\frac{(1-\phi^2)(\tilde{\alpha}_1 - \boldsymbol{x}_1'\boldsymbol{\beta})^2}{2\sigma^2}\right], \tag{39}$$

$$p(\tilde{\alpha}_i|\tilde{\alpha}_{i-1},\boldsymbol{\beta},\phi,\sigma^2,X) = \frac{1}{\sqrt{2\pi\sigma^2}}\exp\left[-\frac{\left\{\tilde{\alpha}_i - \left((\boldsymbol{x}_i' - \phi\boldsymbol{x}_{i-1}')\boldsymbol{\beta} + \phi\tilde{\alpha}_{i-1}\right)\right\}^2}{2\sigma^2}\right]. \tag{40}$$

Then, the joint posterior distribution of θ for Equations (35) and (36) is given by

$$p(\theta|\tilde{\boldsymbol{\alpha}},\boldsymbol{y},X) \propto \prod_{i=1}^{n} p(y_i|\tilde{\alpha}_i,\gamma)p(\tilde{\boldsymbol{\alpha}}|\boldsymbol{\beta},\phi,\sigma^2,X)p(\boldsymbol{\beta})p(\gamma)p(\phi)p(\sigma^2) \tag{41}$$

As with the NCP form, because the joint posterior distribution in Equation (41) cannot be obtained analytically, we employed the MCMC method to estimate it numerically. Then, let us derive the conditional posterior distributions of the parameters in order to perform MCMC with CP.

A.3. CP forms of the conditional posterior distributions

A.3.1. Regression coefficient $\boldsymbol{\beta}$

The conditional posterior distribution of β is given by

$$\begin{aligned} p(\boldsymbol{\beta}|\tilde{\boldsymbol{\alpha}},\phi,\sigma^2,X) &\propto p(\tilde{\boldsymbol{\alpha}}|\boldsymbol{\beta},\phi,\sigma^2,X)p(\boldsymbol{\beta}) \\ &\propto \exp\left[-\frac{1}{2\sigma^2}(\tilde{\boldsymbol{\alpha}} - X\boldsymbol{\beta})'V(\tilde{\boldsymbol{\alpha}} - X\boldsymbol{\beta})' - \frac{1}{2}(\boldsymbol{\beta} - \boldsymbol{\mu}_\beta)'\Sigma_\beta(\boldsymbol{\beta} - \boldsymbol{\mu}_\beta)\right]. \end{aligned}$$

By completing the square for the exponential with respect to $\boldsymbol{\beta}$, we obtain

$$\begin{aligned} &-\frac{1}{2\sigma^2}(\tilde{\boldsymbol{\alpha}} - X\boldsymbol{\beta})'V(\tilde{\boldsymbol{\alpha}} - X\boldsymbol{\beta})' - \frac{1}{2}(\boldsymbol{\beta} - \boldsymbol{\mu}_\beta)'\Sigma_\beta(\boldsymbol{\beta} - \boldsymbol{\mu}_\beta) \\ &= -\frac{1}{2}\left(\frac{1}{\sigma^2}\boldsymbol{\beta}'X'VX\boldsymbol{\beta} - \frac{1}{\sigma^2}\boldsymbol{\beta}'X'V\alpha - \frac{1}{\sigma^2}\tilde{\boldsymbol{\alpha}}'VX\boldsymbol{\beta} + \boldsymbol{\beta}'\Sigma_\beta\boldsymbol{\beta} - \boldsymbol{\beta}'\Sigma_\beta\boldsymbol{\mu}_\beta - \boldsymbol{\mu}'\Sigma_\beta\boldsymbol{\beta}\right) + C \\ &= -\frac{1}{2}\left[\boldsymbol{\beta}'\left(\frac{1}{\sigma^2}X'VX + \Sigma_\beta\right)\boldsymbol{\beta} - \left(\boldsymbol{\beta}'\left(\frac{1}{\sigma^2}X'V\tilde{\boldsymbol{\alpha}} + \Sigma_\beta\boldsymbol{\mu}_\beta\right) + \left(\frac{1}{\sigma^2}X'V\tilde{\boldsymbol{\alpha}} + \Sigma_\beta\boldsymbol{\mu}_\beta\right)'\boldsymbol{\beta}\right)\right] + C. \end{aligned} \tag{42}$$

From Equation (42), the conditional posterior distribution of $\boldsymbol{\beta}$ is given by

$$\boldsymbol{\beta} \sim \text{Normal}\left(\tilde{\boldsymbol{\mu}}_\beta, \tilde{\Sigma}_\beta\right), \tag{43}$$

where

$$\tilde{\Sigma}_\beta = \left(\frac{1}{\sigma^2}X'VX + \Sigma_\beta\right)^{-1}, \quad \tilde{\boldsymbol{\mu}}_\beta = \tilde{\Sigma}_\beta\left(\frac{1}{\sigma^2}X'V\tilde{\boldsymbol{\alpha}} + \Sigma_\beta\tilde{\boldsymbol{\mu}}_\beta\right).$$

A.3.2. Shape parameter γ

By replacing $\alpha_i + \boldsymbol{x}_i'\boldsymbol{\beta}$ with $\tilde{\alpha}_i$, Equations (6) and (27) become

$$\log p(y_i|\tilde{\alpha}_i, \gamma) = \log\gamma - \log y_i + \gamma(\log y_i - \tilde{\alpha}_i) - \exp(\gamma(\log y_i - \tilde{\alpha}_i)), \tag{44}$$

$$\tilde{f}(\gamma) \equiv \sum_{i=1}^{n} \log p(y_i|\tilde{\alpha}_i, \gamma) + \log p(\gamma) + \text{constant}. \tag{45}$$

Then, the second-order Taylor expansion of Equation (27) with respect to γ in the neighborhood of $\gamma^* > 0$ becomes

$$\tilde{f}(\gamma) \approx \tilde{f}(\gamma^*) + \tilde{g}(\gamma^*)(\gamma - \gamma^*) - \frac{1}{2}\tilde{q}(\gamma^*)(\gamma - \gamma^*)^2, \tag{46}$$

where

$$\begin{aligned}
\tilde{g}(\gamma^*) &\equiv \nabla_\gamma \tilde{f}(\gamma^*) \\
&= \frac{n}{\gamma^*} + \sum_{i=1}^{n}\left(\tilde{u}_i - \tilde{u}_i e^{\gamma^* u_i}\right) + \frac{a_\gamma - 1}{\gamma^*} - b_\gamma, \\
\tilde{q}(\gamma^*) &\equiv -\nabla_\gamma^2 \tilde{f}(\gamma^*) \\
&= \frac{n}{\gamma^{*2}} + \sum_{i=1}^{n} \tilde{u}_i^2 e^{\gamma^* \tilde{u}_i} + \frac{a_\gamma - 1}{\gamma^{*2}}, \\
\tilde{u}_i &\equiv \log y_i - \tilde{\alpha}_i, \quad i \in \{1, \dots, n\}.
\end{aligned}$$

By completing the square of Equation (46), we obtain the following proposal distribution:

$$\gamma \sim \text{Normal}\left(\tilde{\mu}_\alpha(\gamma^*), \tilde{\sigma}_\gamma^2(\gamma^*)\right), \tag{47}$$

where

$$\tilde{\sigma}_\gamma^2(\gamma^*) = \frac{1}{\tilde{q}(\gamma^*)}, \quad \tilde{\mu}_\gamma(\gamma^*) = \gamma^* + \frac{\tilde{g}(\gamma^*)}{\tilde{q}(\gamma^*)},$$

for sampling γ by the MH algorithm.

A.3.3. AR(1) coefficient ϕ

By replacing α_i with $\tilde{\alpha}_i - \boldsymbol{x}_i'\boldsymbol{\beta}$ in Equation (31), we obtain

$$\phi \sim \text{Normal}\left(\tilde{\Sigma}_\phi \sum_{i=2}^{n}(\tilde{\alpha}_i - \boldsymbol{x}_i'\boldsymbol{\beta})(\tilde{\alpha}_{i-1} - \boldsymbol{x}_{i-1}'\boldsymbol{\beta}), \sigma^2\tilde{\Sigma}_\phi\right), \tag{48}$$

where

$$\tilde{\Sigma}_\phi = \left(\sum_{i=2}^{n-1}(\tilde{\alpha}_i - \boldsymbol{x}_i'\boldsymbol{\beta})^2\right)^{-2}$$

is the proposal distribution for ϕ in the MH algorithm.

A.3.4. Variance σ^2 (CP form)

By replacing α_i with $\tilde{\alpha}_i - \boldsymbol{x}_i'\boldsymbol{\beta}$ in Equation (33), we obtain

$$\sigma^2|\boldsymbol{y}, X, \tilde{\boldsymbol{\alpha}}, \boldsymbol{\beta}, \sim \text{Inv. Gamma}\left(a_\sigma + \frac{n}{2}, b_\sigma + \frac{1}{2}\left(\tilde{\boldsymbol{\alpha}} - X'\boldsymbol{\beta}\right)' V \left(\tilde{\boldsymbol{\alpha}} - X'\boldsymbol{\beta}\right)\right) \tag{49}$$

as the conditional posterior distribution of σ^2.

A.4. ASIS Application to MCMC

ASIS is simple to apply: the NCP and CP sampling schemes are interweaved alternately. Note that the random number generation for sampling is adopted for only one of the NCP and CP forms. Because the correct statistical estimation is possible regardless of which form is chosen, we applied the random number generation for sampling to the CP form.

Outline of the sampling scheme (ASIS)

Step 0: Initialize $(\boldsymbol{\alpha}^{(0)}, \boldsymbol{\beta}^{(0)}, \gamma^{(0)}, \phi^{(0)}, \sigma^{2(0)})$ and set the counter $r = 0$.

Step 1.1: Generate $\boldsymbol{\alpha}^{(r+1)}$ from $p(\boldsymbol{\alpha}|\boldsymbol{\beta}^{(r)}, \gamma^{(r)}, \phi^{(r)}, \sigma^{2(r)}, \boldsymbol{y}, X)$ from Equation (18).

Step 1.2: Generate $\boldsymbol{\beta}^{(r+0.5)}$ from $p(\boldsymbol{\beta}|\boldsymbol{\alpha}^{(r+1)}, \gamma^{(r)}, \phi^{(r)}, \sigma^{2(r)}, \boldsymbol{y}, X)$ from Equation (26).

Step 1.3: Generate $\gamma^{(r+0.5)}$ from $p(\gamma|\boldsymbol{\alpha}^{(r+1)}, \boldsymbol{\beta}^{(r+0.5)}, \phi^{(r)}, \sigma^{2(r)}, \boldsymbol{y}, X)$ from Equation (29).

Step 1.4: Generate $\phi^{(r+0.5)}$ from $p(\phi|\boldsymbol{\alpha}^{(r+1)}, \boldsymbol{\beta}^{(r+0.5)}, \gamma^{(r+0.5)}, \sigma^{2(r)}, \boldsymbol{y}, X)$ from Equation (31).

Step 1.5: Generate $\sigma^{2(r+0.5)}$ from $p(\sigma^2|\boldsymbol{\alpha}^{(r+1)}, \boldsymbol{\beta}^{(r+0.5)}, \gamma^{(r+0.5)}, \phi^{(r+0.5)}, \boldsymbol{y}, X)$ from Equation (33).

Step 2.1: Calculate $\tilde{\boldsymbol{\alpha}}^{(r+1)} = \boldsymbol{\alpha}^{(r+1)} - X\boldsymbol{\beta}^{(r+0.5)}$.

Step 2.2: Generate $\boldsymbol{\beta}^{(r+1)}$ from $p(\boldsymbol{\beta}|\tilde{\boldsymbol{\alpha}}^{(r)}, \gamma^{(r+0.5)}, \phi^{(r+0.5)}, \sigma^{2(r+0.5)}, \boldsymbol{y}, X)$ from Equation (43).

Step 2.3: Generate $\gamma^{(r+1)}$ from $p(\gamma|\tilde{\boldsymbol{\alpha}}^{(r+1)}, \boldsymbol{\beta}^{(r+1)}, \phi^{(r+0.5)}, \sigma^{2(r+0.5)}, \boldsymbol{y}, X)$ from Equation (47).

Step 2.4: Generate $\phi^{(r+1)}$ from $p(\phi|\tilde{\boldsymbol{\alpha}}^{(r+1)}, \boldsymbol{\beta}^{(r+1)}, \gamma^{(r+1)}, \sigma^{2(r+0.5)}, \boldsymbol{y}, X)$ from Equation (48).

Step 2.5: Generate $\sigma^{2(r+1)}$ from $p(\sigma^2|\tilde{\boldsymbol{\alpha}}^{(r+1)}, \boldsymbol{\beta}^{(r+1)}, \gamma^{(r+1)}, \phi^{(r+1)}, \boldsymbol{y}, X)$ from Equation (49).

Step 3: Let $r = r + 1$, and go to **Step 1-1** until the burn-in iterations are completed.

Step 4: Reset the counter $r = 0$, and repeat **Step 1.1–2.5** R times to obtain the Monte Carlo sample $(\boldsymbol{\alpha}^{(r)}, \boldsymbol{\beta}^{(r)}, \gamma^{(r)}, \phi^{(r)}, \sigma^{2(r)})_{r=1}^{R}$.

Author contributions

Makoto Nakakita: Conceptualization, Software, Data curation, Formal analysis, Funding acquisition, Validation, Investigation, Visualization, Methodology, Writing – original draft, Writing – review and editing.

Teruo Nakatsuma: Conceptualization, Software, Resources, Supervision, Funding acquisition, Methodology, Writing – review and editing, Project administration.

Use of AI tools declaration

The authors declare they have not used Artificial Intelligence (AI) tools in the creation of this article.

Acknowledgement

This research was funded by JSPS KAKENHI Grant Numbers JP23K18819, JP20H00088.

Conflict of interest

All authors declare no conflicts of interest in this paper.

References

Aharon DY, Qadan M (2019) Bitcoin and the day-of-the-week effect. *Finance Res Lett* 31. https://doi.org/10.1016/j.frl.2018.12.004

Bauwens L, Veredas D (2004) The stochastic conditional duration model: a latent variable model for the analysis of financial durations. *J Econom* 119: 381–412. https://doi.org/10.1016/S0304-4076(03)00201-X

Ben Omrane W, Houidi F, Savaser T (2023) Macroeconomic news and intraday seasonal volatility in the cryptocurrency markets. *Appl Econ* 56: 4594–4610. https://doi.org/10.1080/00036846.2023.2212970

Bernstein S (1912) Demonstration of a theorem of weierstrass based on the calculus of probabilities. *Commun Kharkov Math Soc* 13: 1–2. Available from: https://www.mn.uio.no/math/english/people/aca/michaelf/translations/bernstein_english.pdf.

Cryptocurrency historical market data. Binance. Available from: http://www.sars-expertcom.gov.hk/english/reports/reports.html.

State of the Blockchain - 2024 Year in Review. Binance. Available from: https://public.bnbstatic.com/reports/2024_EOY_Report.pdf.

Bollerslev T (1986) Generalized autoregressive conditional heteroskedasticity. *J Econom* 31: 307–327. https://doi.org/10.1016/0304-4076(86)90063-1

Bollerslev T, Litvinova J, Tauchen G (2006) Leverage and volatility feedback effects in high-frequency data. *J Financ Econom* 4: 353–384. https://doi.org/10.1093/jjfinec/nbj014

Bouteska A, Abedin MZ, Hájek P, et al. (2024) Cryptocurrency price forecasting – a comparative analysis of ensemble learning and deep learning methods. *Int Rev Financ Anal* 92: 103055. https://doi.org/10.1016/j.irfa.2023.103055

Brini A, Lenz J (2024) A comparison of cryptocurrency volatility-benchmarking new and mature asset classes. *Financ Innov* 10: 122. https://doi.org/10.1186/s40854-024-00646-y

Chen J (2023) Analysis of bitcoin price prediction using machine learning. *J Risk Financ Manage* 16: 51. https://doi.org/10.3390/jrfm16010051

Christin N (2013) Traveling the silk road: a measurement analysis of a large anonymous online marketplace. *In Proceedings of the 22nd International Conference on World Wide Web*: 213–224. https://doi.org/10.1145/2488388.2488408

Chu J, Chan S, Nadarajah S, et al. (2017) Garch modelling of cryptocurrencies. *J Risk Financ Manage* 10: 17. https://doi.org/10.3390/jrfm10040017

Cohen G (2023) Intraday algorithmic trading strategies for cryptocurrencies. *Rev Quant Finance Account* 61: 395–409. https://doi.org/10.1007/s11156-023-01139-2

Derbentsev, Matviychuk A, Soloviev VN (2020) Forecasting of Cryptocurrency Prices Using Machine Learning. *In Advanced Studies of Financial Technologies and Cryptocurrency Markets*, Springer, Singapore, 211–231. https://doi.org/10.1007/978-981-15-4498-9_12

Engle RF (1982) Autoregressive conditional heteroscedasticity with estimates of the variance of united kingdom inflation. *Econometrica* 50: 987–1007. https://doi.org/10.2307/1912773

Engle RF, Russell JR (1999) Autoregressive conditional duration: A new model for irregularly spaced transaction data. *Econometrica* 66: 1127–1162. https://doi.org/10.2307/2999632

Eross A, McGroarty F, Urquhart A, et al. (2019) The intraday dynamics of bitcoin. *Res Int Bus Finance* 49: 71–81. https://doi.org/10.1016/j.ribaf.2019.01.008

Georgoula I, Pournarakis D, Bilanakos C, et al. (2015) Using Time-Series and Sentiment Analysis to Detect the Determinants of Bitcoin Prices. *In MCIS 2015 Proceedings*: 20. https://doi.org/10.2139/ssrn.2607167

Gradojevic N, Tsiakas I (2021) Volatility cascades in cryptocurrency trading. *J Empirical Finance* 62: 252–265. https://doi.org/10.1016/j.jempfin.2021.04.005

Hajek P, Hikkerova L, Sahut JM (2023) How well do investor sentiment and ensemble learning predict bitcoin prices? *Res Int Bus Finance* 64: 101836. https://doi.org/10.1016/j.ribaf.2022.101836

Inuduka T, Yokose A, Managi S (2024) Influencing cryptocurrency: analyzing celebrity sentiments on x (formerly twitter) and their impact on bitcoin prices. *Digital Finance* 6: 379–426. https://doi.org/10.1007/s42521-024-00106-3

Iqbal M, Iqbal MS, Jaskani FH, et al. (2021) Time-series prediction of cryptocurrency market using machine learning techniques. *EAI Endorsed Transactions on Creative Technologies* 8: 170286. https://doi.org/10.4108/eai.7-7-2021.170286

Jing L, Kang, Y (2024) Automated cryptocurrency trading approach using ensemble deep reinforcement learning: Learn to understand candlesticks. *Expert Syst Appl* 237: 121373. https://doi.org/10.1016/j.eswa.2023.121373

Khurana SS, Singh P, Garg NK (2023) Revolutionize ai trading bots with automl-based multi-timeframe bitcoin price prediction. *SN Comput Sci* 4: 492. https://doi.org/10.1007/s42979-023-01941-8

Kim G, Shin DH, Choi JG, et al. (2022) A deep learning-based cryptocurrency price prediction model that uses on-chain data. *IEEE Access* 10: 56232–56248. https://doi.org/10.1109/ACCESS.2022.3177888

Madan I, Saluja S, Zhao A (2014) Automated Bitcoin Trading via Machine Learning Algorithms. Available from: https://cs229.stanford.edu/proj2014/Isaac%20Madan,%20Shaurya%20Saluja,%20Aojia%20Zhao,Automated%20Bitcoin%20Trading%20via%20Machine%20Learning%20Algorithms.pdf.

Maleki N, Nikoubin A, Rabbani M, et al. (2023) Bitcoin price prediction based on other cryptocurrencies using machine learning and time series analysis. *Sci Iran* 30: 285–301. https://doi.org/10.24200/sci.2020.55034.4040

Malladi RK, Dheeriya PL (2021) Time series analysis of cryptocurrency returns and volatilities. *J Econ Finance* 45: 75–94. https://doi.org/10.1007/s12197-020-09526-4

Men Z, Kolkiewicz A, Wirjanto TS (2015) Bayesian inference of asymmetric stochastic conditional duration models. *J Stat Comput Simul* 86: 1295–1319. Available from: https://ssrn.com/abstract=2241082.

Moustafa H, Malli M, Hazimeh H (2022) Real-time bitcoin price tendency awareness via social media content tracking. *In 2022 10th International Symposium on Digital Forensics and Security (ISDFS)*: 1–6. https://doi.org/10.1109/ISDFS55398.2022.9800793

Nakakita M, Nakatsuma T (2021) Bayesian analysis of intraday stochastic volatility models of high-frequency stock returns with skew heavy-tailed errors. *J Risk Financ Manage* 14: 145. https://doi.org/10.3390/jrfm14040145

Nakamoto S (2008) Bitcoin: A peer-to-peer electronic cash system. Available from: https://bitcoin.org/bitcoin.pdf.

Omori Y, Chib S, Shephard N, et al. (2007) Stochastic volatility with leverage: Fast and efficient likelihood inference. *J Econom* 140: 425–449. https://doi.org/10.1016/j.jeconom.2006.07.008

Otabek S, Choi J (2022) Twitter attribute classification with q-learning on bitcoin price prediction. *IEEE Access* 10: 96136–96148. https://doi.org/10.1109/ACCESS.2022.3205129

Oyedele AA, Ajayi Ao, Oyedele LO, et al. (2023) Performance evaluation of deep learning and boosted trees for cryptocurrency closing price prediction. *Expert Syst Appl* 213: 119233. https://doi.org/10.1016/j.eswa.2022.119233

Politis A, Doka K, Koziris N (2021) Ether price prediction using advanced deep learning models. *In 2021 IEEE International Conference on Blockchain and Cryp- tocurrency (ICBC)*: 1–3. https://doi.org/10.1109/ICBC51069.2021.9461061

Poongodi M, Vijayakumar V, Chilamkurti N (2020) Bitcoin price prediction using ARIMA model. *Int J Internet Technol Secured Trans* 10: 396–406. https://doi.org/10.1504/IJITST.2020.108130

Qadan M, Aharon DY, Eichel R (2022) Seasonal and Calendar Effects and the Price Efficiency of Cryptocurrencies. *Finance Res Lett* 46: 102354. https://doi.org/10.1016/j.frl.2021.102354

Ranjan S, Kayal P, Saraf M (2023) Bitcoin Price Prediction: A Machine Learning Sample Dimension Approach. *Comput Econ* 61: 1617–1636. https://doi.org/10.1007/s10614-022-10262-6

Shah D, Zhang K (2014) Bayesian regression and bitcoin. *In 2014 52nd Annual Allerton Conference on Communication, Control, and Computing (Allerton)*: 409–414. https://doi.org/10.1109/ALLERTON.2014.7028484

Shanaev S, Ghimire B (2022) A generalised seasonality test and applications for cryptocurrency and stock market seasonality. *Q Rev Econ Finance* 86: 172–185. https://doi.org/10.1016/j.qref.2022.07.002

Shepard N, Pitt MK (1997) Likelihood analysis of non-Gaussian measurement time series. *Biometrika* 84: 653–667. https://doi.org/10.1093/biomet/84.3.653

Spiegelhalter DJ, Best NG, Carlin BP, et al. (2002) Bayesian Measures of Model Complexity and Fit. *J R Stat Soc B* 64: 583–639. https://doi.org/10.1111/1467-9868.00353

Su F, Wang X, Yuan Y (2022) The intraday dynamics and intraday price discovery of bitcoin. *Res Int Bus Finance* 60: 101625. https://doi.org/10.1016/j.ribaf.2022.101625

Tanwar S, Patel SN, Patel JR, et al. (2021) Deep learning-based cryptocurrency price prediction scheme with inter-dependent relations. *IEEE Access* 9: 138633–138646. https://doi.org/10.1109/ACCESS.2021.3117848

Thekke R, Mishra A, Abraham B (2016) Estimation, filtering and smoothing in the stochastic conditional duration model: an estimating function approach. *Stat* 5: 11–21. https://doi.org/10.1002/sta4.101

Toyabe T, Nakakita M, NakatsumaT (2024) Bayesian analysis of stochastic conditional duration models with intraday and intradeferred future seasonalities in high-frequency commodity market. *In 2024 15th IIAI International Congress on Advanced Applied Informatics (IIAI-AAI)*: 305–311. https://doi.org/10.1109/IIAI-AAI63651.2024.00064

Toyabe T, Nakatsuma T (2022) Stochastic conditional duration model with intraday seasonality and limit order book information. *J Risk Financ Manage* 15: 470. https://doi.org/10.3390/jrfm15100470

Tran M, Pham-Hi D, Bui M (2023) Optimizing automated trading systems with deep reinforcement learning. *Algorithms* 16: 23. https://doi.org/10.3390/a16010023

Tsang EPK (2021) Directional change for handling tick-to-tick data. *J Chin Econ Bus Stud* 20: 171–182. https://doi.org/10.1080/14765284.2021.1989883

Tsang EPK, Tao R, Serguieva A, et al. (2016) Profiling high-frequency equity price movements in directional changes. *Quant Finance* 17: 217–225. https://doi.org/10.1080/14697688.2016.1164887

Umar Z, Gubareva M (2020) A time–frequency analysis of the impact of the covid-19 induced panic on the volatility of currency and cryptocurrency markets. *J Behav Exp Finance* 28: 100404. https://doi.org/10.1016/j.jbef.2020.100404

Wang Y, Andreeva G, Martin-Barragan B (2023) Machine learning approaches to forecasting cryptocurrency volatility: Considering internal and external determinants. *Int Rev Financ Anal* 90: 102914. https://doi.org/10.1016/j.irfa.2023.102914

Washington PB, Gali P, Rustam F, et al. (2023) Analyzing influence of covid-19 on crypto & financial markets and sentiment analysis using deep ensemble model. *PLOS ONE* 18: e0286541. https://doi.org/10.1371/journal.pone.0286541

Watanabe T, Omori Y (2004) A multi-move sampler for estimating non-gaussian time series models: Comments on shephard & pitt (1997). *Biometrika* 19: 246–248. https://doi.org/10.1093/biomet/91.1.246

Xu D, Knight J, Wirjanto TS (2010) Asymmetric stochastic conditional duration model–a mixture-of-normal approach. *J Financ Econom* 9: 469–488. https://doi.org/10.1093/jjfinec/nbq026

Yu Y, Meng X-L (2011) To center or not to center: That is not the question–an ancillarity-sufficiency interweaving strategy (asis) for boosting mcmc efficiency. *J Comput Graphical Stat* 20: 531–570. https://doi.org/10.1198/jcgs.2011.203main